Disruption of coronin 1 signaling in T cells promotes allograft tolerance while maintaining anti-pathogen immunity

Rajesh Jayachandran*[1], Aleksandra Gumienny[1], Beatrice Bolinger[1], Sebastian Ruehl[1], Mathias Jakob Lang[1], Geoffrey Fucile[4], Saumyabrata Mazumder[1], Vincent Tchang[1], Anne-Kathrin Woischnig[2], Michael Stiess[1], Gabriele Kunz[1], Beatrice Claudi[1], Mathias Schmaler[2], Kerstin Siegmund[1], Jianping Li[5], Simone Dertschnig[2], George Holländer[2,6], Eva Medina[7], Urs Karrer[8], Despina Moshous[9,10], Dirk Bumann[1], Nina Khanna[2,3], Simona W Rossi[2] and Jean Pieters*[1]

[1]Biozentrum and [2]Department of Biomedicine, University of Basel, University Hospital of Basel, Basel, Switzerland; [3]Division of Infectious Diseases, University and University Hospital of Basel, Switzerland; [4]Swiss Institute of Bioinformatics, sciCORE Computing Center, University of Basel, Basel, Switzerland; [5]Novartis, Basel, Switzerland; [6]Department of Paediatrics, University of Oxford, United Kingdom; [7]Helmholtz Center for Infection Research, Braunschweig, Germany; [8]Division of Infectious Diseases, [8]Department of Medicine, Cantonal Hospital of Winterthur, Winterthur, Switzerland; [9]Université Paris Descartes–Sorbonne Paris Cité, Institut Imagine, Paris, France and APHP Hôpital Universitaire Necker-Enfants Malades, Unité d'Immunologie-Hématologie et Rhumatologie Pédiatrique, Paris, France;

Present addresses: KS: Department for Pharmacology and Genetics, Medical University of Innsbruck, Innsbruck, Austria; MJL: Thermo Scientific, Basel, Switzerland; SM: Premas Biotech, New Delhi, India.

*Correspondence: JP (Lead Contact)/RJ, Phone: + 41 61 207 14 94, Fax: + 41 61 207 21 48,
Email: jean.pieters@unibas.ch/rajesh.jayachandran@unibas.ch

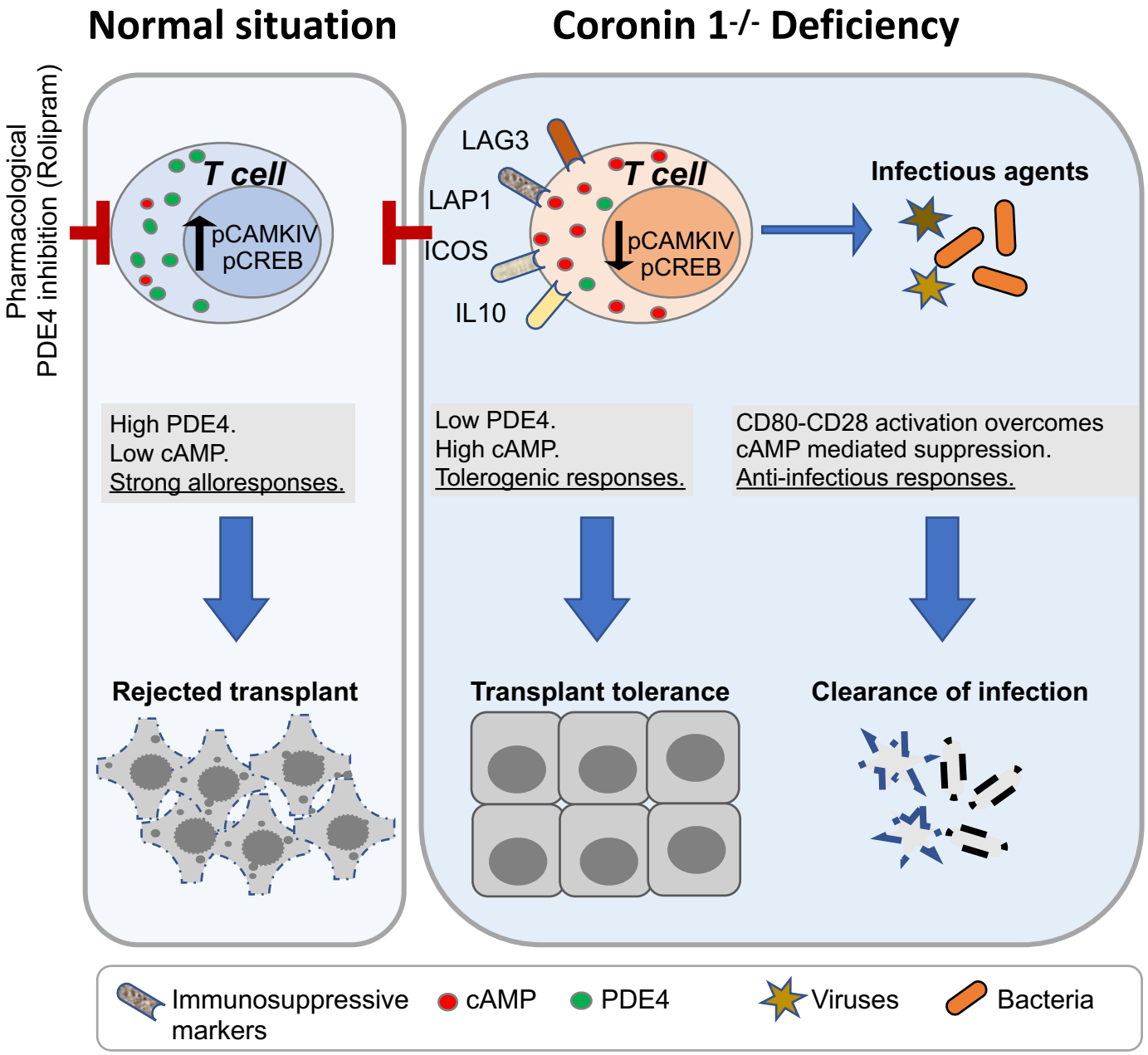
Normal situation
Coronin 1-/- Deficiency
Pharmacological
PDE4 inhibition (Rolipram)
T cell
pCAMKIV
pCREB
LAG3
LAP1
ICOS
IL10
T cell
pCAMKIV
pCREB
Infectious agents
High PDE4.
Low cAMP.
Strong alloresponses.
Low PDE4.
High cAMP.
Tolerogenic responses.
CD80-CD28 activation overcomes
cAMP mediated suppression.
Anti-infectious responses.
Rejected transplant
Transplant tolerance
Clearance of infection
Immunosuppressive markers
cAMP
PDE4
Viruses
Bacteria

Summary

The ability of the immune system to discriminate self from non-self is essential for eradicating microbial pathogens but is also responsible for allograft rejection. Whether it is possible to selectively suppress alloresponses while maintaining anti-pathogen immunity remains unknown. We found that mice deficient in coronin 1, a regulator of naïve T cell homeostasis, fully retained allografts while maintaining T cell-specific responses against microbial pathogens. Mechanistically, coronin 1-deficiency increased cyclic adenosine monophosphate (cAMP) concentrations to suppress allo-specific T cell responses. Costimulation induced on microbe-infected antigen presenting cells was able to overcome cAMP-mediated immunosuppression to maintain anti-pathogen immunity. *In vivo* pharmacological modulation of this pathway or a prior transfer of coronin 1-deficient T cells actively suppressed allograft rejection. These results define a coronin 1-dependent regulatory axis in T cells important for allograft rejection and suggest that modulation of this pathway may be a promising approach to achieve long-term acceptance of mismatched allografts.

Introduction

The ability of a vertebrate host to initiate T cell responses towards pathogenic microbes relies on the appropriate recognition of antigenic peptides presented on antigen presenting cells (APC's) via an individual's own Major Histocompatibility Complex (MHC) molecules (Zinkernagel and Doherty, 1979). The MHC molecules are by far the most polymorphic known, possibly having evolved to prevent pathogens from escaping immune detection while avoiding reactivity against 'self' (Doherty and Zinkernagel, 1975). To achieve this, T cells are selected in the thymus in order to delete auto-reactive T cells and allow only those cells to reach the periphery that lack reactivity towards self and can recognize foreign peptides in the context of self-MHC (Doherty and Zinkernagel, 1975; Goldrath and Bevan, 1999; Huseby et al., 2005). The polymorphic nature of the MHC molecules allows the recognition of a large variety of antigenic peptides, but has the consequence that, with the exception of identical twins, there are rarely two individuals who carry exactly the same set of MHC genes and molecules thus resulting in a virtual inability to accept allografts; this problem is further exacerbated by the existence of minor histocompatibility antigens (Goulmy et al., 1996).

T cells that are exported from the thymus are maintained in the periphery through pro-survival signals that are delivered through the T cell receptor (TCR) by self-peptide:MHC interaction as well as interleukin-7 signaling (Surh and Sprent, 2008). Recent work has suggested the presence of a third axis required for naïve T cell homeostasis that relies on the activity of the WD repeat protein coronin 1 (also known as P57 or Tryptophan Aspartate containing COat (TACO) protein) (Foger et al., 2006; Mueller et al., 2008; Shiow et al., 2008). In the absence of coronin 1, naïve

T cells are depleted while other leukocytes remain functional and exist in normal numbers, although coronin 1 may play a role in the functionality of natural killer cells and neutrophils (Arandjelovic et al., 2010; Combaluzier et al., 2009; Combaluzier and Pieters, 2009; Haraldsson et al., 2008; Jayachandran et al., 2007; Mace and Orange, 2014; Pick et al., 2017; Siegmund et al., 2013; Tchang et al., 2017; Westritschnig et al., 2013). Coronin 1 is dispensable for T cell differentiation, selection and export to secondary lymphoid organs (Lang et al., 2017), suggesting that coronin 1 mediates T cell homeostasis through an as yet undefined mechanism.

Here, we describe an essential role for coronin 1 in allograft rejection via the modulation of the phosphodiesterase 4-CREB-CaMKIV pathway in T cells. We found that coronin 1 maintains appropriate levels of cAMP, similar to its role in regulating the cAMP-protein kinase A pathway in neurons and *Dictyostelium* (via its orthologue coronin A, (Jayachandran et al., 2014; Vinet et al., 2014)). Suppression was specific for alloresponses, since infection-mediated CD28 ligation through CD80 could overcome cAMP-mediated suppression of T cell responses. Finally, we describe that this pathway could be targeted *in vivo*, suggesting a potential for interfering with this pathway to achieve long-term graft acceptance without compromising immunity to infections.

Results

Mice lacking coronin 1 are tolerant of allografts but maintain immunity against microbial pathogens

Deletion of coronin 1 in mice results in a specific and selective depletion of peripheral mature naïve T cells. To understand the relative importance of the coronin 1-dependent T cell subset for alloresponses versus immunity towards pathogenic microbes, mice lacking coronin 1 were subjected to transplantation and microbial challenges.

For transplantations, MHC mismatched donor hearts (BALB/c, I-A^d) were transplanted into C57BL/6 wild-type (WT) or coronin 1-deficient (*Coro1a*$^{-/-}$, see also Pieters et al., 2013 for nomenclature) mice (I-A^b) by grafting BALB/c cardiac allografts onto the abdominal aorta (Niimi 2001). While allografts were rapidly rejected in all WT recipients by day 8, in *Coro1a*$^{-/-}$ recipients BALB/c hearts remained fully functional until study termination at 106 days (Figure 1A-C). Histology of the BALB/c hearts revealed severe vasculopathy in WT recipients (on day 8), whereas *Coro1a*$^{-/-}$ mice showed only minimal vascular changes (on day 106, with beating hearts) (Figure 1B and C).

One of the most challenging organs in terms of allograft retention is skin because of its highly immunogenic nature (Richters et al., 2005). To analyze a role for coronin 1 in skin graft rejection, skin grafts representing both major (H2-bm12 (I-A^{bm12})); Figure 1D-F) (McKenzie et al., 1979) or minor histocompatibility antigen-mismatch (BALB/c^d) (Figure 1G and S1A) were transplanted onto either C57BL/6 WT or *Coro1a*$^{-/-}$ mice (I-A^b). Similar to the results described above, *Coro1a*$^{-/-}$ mice allowed long-term retention of the skin allografts whereas all WT recipients rejected rapidly (Figure 1D-G and Figure 1SB-D). Furthermore, in a non-irradiated haploidentical hematopoietic transplantation model (B6 (I-A^b) ->

BDF_1 ($I\text{-}A^{bd}$)), transfer of *Coro1a*$^{-/-}$ T cells did not result in acute graft versus host disease (Figure S1E and F) consistent with previous data from an irradiated model (Fulton et al., 2014; Krenger et al., 2000b). Together these results suggest the occurrence of long-term allograft acceptance in the absence of coronin 1.

In contrast to the tolerance towards allografts, deficiency of coronin 1 allowed appropriate responses against a range of pathogenic microbial challenges: when infected with *S. aureus* or *C. albicans*, *Coro1a*$^{-/-}$ mice cleared the microbial load as observed for WT mice (Figure 2A,B and Figure S2A,B), and similar results were seen with intravenous administration of *S. aureus* (Figure S2C), a model for persistent infection (Ziegler et al., 2011). Infection with virulent *S. typhimurium* resulted in comparable mouse survival kinetics and bacterial burden in spleen and liver (Figure 2C and Figure S2E). To assess T cell-specific responses, we generated *Coro1a*$^{-/-}$ OTII transgenic mice whose T cells express a T cell receptor that specifically recognizes an ovalbumin peptide in the context of $I\text{-}A^b$. Upon infection with ovalbumin-expressing *S. typhimurium*, both WT and *Coro1a*$^{-/-}$ OTII T cells underwent specific proliferation and expansion, suggesting that *Coro1a*$^{-/-}$ T cells could recognize and mount adaptive immune responses. Both genotypes could be protectively vaccinated against virulent *Salmonella*, a process that depends on $CD4^+$-specific T cell responses (Kupz et al., 2014; Ravindran and McSorley, 2005) (Figure 2E). The responses against a challenge with murine cytomegalovirus (the virulent MCMV- Δ M157 strain that does not activate NK cells (Bubic et al., 2004; Walton et al., 2008)) and whose control is critically dependent on T cell responses (Klenerman and Oxenius, 2016; Verma et al., 2015) was similar in liver and lungs, with a slight delay in clearance in spleen

and salivary glands (Figure 2F) accompanied by the occurrence of specific T cell responses (Figure 2G). Mice lacking coronin 1 showed an overall health similar to WT mice, including life expectancy, absence of malignancies, comparable composition of viral, bacterial and parasitic flora (Table S1,2, Figure S2D,F). These data suggest that the observed allograft acceptance is not due to an overall reduction in T cell effector function but rather a T cell-intrinsic defect when reacting to major and minor alloantigens.

Coro1a$^{-/-}$ CD4^{+} T cells induce tolerance in vivo

The tolerance towards allografts in the absence of coronin 1 could be a result of the paucity of T cells, an amplification of the regulatory T cell (Treg) response or an active induction of tolerance by *Coro1a$^{-/-}$* T cells. To assess if the absence of rejection in *Coro1a$^{-/-}$* mice was due to a paucity of naive T cell numbers, *Rag2$^{-/-}$* mice carrying a major mismatched allograft were adoptively transferred with varying numbers of *Coro1a$^{-/-}$* CD4^{+} T cells (up to 1 million) or 20,000 WT CD4^{+} T cells. While transfer of 20,000 WT CD4^{+} T cells resulted in rapid rejection, none of the *Rag2$^{-/-}$* mice that received *Coro1a$^{-/-}$* CD4^{+} T cells rejected the allografts (Figure S3A). Furthermore, while transfer of 20,000 WT T cells (CD4^{+}CD25^{-}) into RAG2$^{-/-}$ mice bearing a minor mismatched graft resulted in rejection, adoptive transfer of up to 10^{6} WT T cells (CD4^{+}CD25^{-}) into minor mismatched allograft-bearing *Cor 1$^{-/-}$* mice did not result in rejection (Figure 3A, S3B,). Similarly, transfer of up to 5 million WT CD4^{+}CD25^{-} T cell into *Coro1a$^{-/-}$* mice did not trigger graft rejection in a major mismatch model (Figure 3B, S3D). The absence of graft rejection was not due to failure of the transferred WT T cells to survive in the *Coro1a$^{-/-}$* environment as these cells remained to be detected at various time points (inset in Figure 3A, 3B and Figure

S3B-E). In both adoptive transfer experiments, the total number of transferred WT cells recovered from *Coro1a*$^{-/-}$ mice was significantly lower than the numbers recovered from *Rag2*$^{-/-}$ mice transferred with equal number of WT T cells (20'000 cells, Figure S3B and S3D) and the T cells were less activated (Figure S3F). These results suggest the presence of an altered milieu that limited the expansion and/or survival of transferred WT T cells in *Coro1a*$^{-/-}$ mice.

Regulatory T (Treg, $CD4^+CD25^+$) cells play an important role in suppression of graft rejection responses (Josefowicz et al., 2012; Sakaguchi et al., 2008; Tang and Bluestone, 2013). To assess if the observed long-term allograft acceptance in *Coro1a*$^{-/-}$ mice was mediated by Treg cells, mice were treated with PC61 antibodies (Figure S4A) that effectively depleted $CD4^+CD25^+$ Treg cells (Figure S4B). Treg cell depletion failed to induce allograft rejection (Figure 3c) suggesting that allograft survival in *Coro1a*$^{-/-}$ mice did not involve allo-reactive Treg cells.

To address this further, *Coro1a*$^{-/-}$ mice carrying minor mismatched allografts were depleted of Treg cells followed by adoptive transfer with 100'000 WT $CD4^+CD25^-$ T cells, and the kinetics of allograft rejection monitored. As a positive control for adoptive cell transfer and cell vitality, *Rag2*$^{-/-}$ mice carrying minor mismatched skin allografts received 20'000 WT $CD4^+CD25^-$ T cells. While grafts were readily rejected by *Rag2*$^{-/-}$ mice post-adoptive transfer of WT T cells (Figure 3D), none of the Treg cell-depleted *Coro1a*$^{-/-}$ mice that received WT $CD4^+$ T cells rejected the skin graft (Figure 3D). We confirmed the presence of transferred WT T cells and efficiency of $CD4^+CD25^+$ T cell depletion by flow cytometry (Figure S4B-D). Principal component analysis (PCA) of the transcriptomes from WT and *Coro1a*$^{-/-}$ T cells revealed that

Coro1a$^{-/-}$ conventional T cells did not cluster with WT conventional T cells and carried a T cell signature distinct from Treg cells, while Treg cells from both genotypes clustered together (Figure 3E), providing further evidence that the absence of coronin 1 does not induce a Treg phenotype. Moreover, *Coro1a*$^{-/-}$ conventional T cells displayed significantly higher levels of immunosuppressive markers (Figure S4E,F) and their co-transfer with WT $CD4^+CD25^-$ T cells into *Rag2*$^{-/-}$ mice actively suppressed homeostatic expansion of WT $CD4^+CD25^-$ T cells *in vivo* (Figure 3F-H) (Tao et al., 2007). These data suggest that the absence of coronin 1 results in long-term allograft acceptance of allografts through suppression of T cell allo-responses independently of $CD4^+CD25^+$ Treg cells.

Coronin 1 in T cells regulates the cAMP-PKA-pCREB pathway

To analyze a possible mechanism for the observed tolerance in the absence of coronin 1, whole transcriptome (RNAseq) analysis was performed on WT and *Coro1a*$^{-/-}$ conventional ($CD4^+CD25^-$) and regulatory ($CD4^+$ $CD25^+$) T cells. Reactome pathway analysis of the differentially regulated genes in conventional *Coro1a*$^{-/-}$ T cells showed regulators of the cyclic adenosine mono phosphate (cAMP) pathway (Figure S5A,B and Table S3), consistent with the recently described capacity of coronin 1 to modulate the cAMP pathway (Jayachandran et al., 2014; Suo et al., 2014). cAMP modulates T cell immune responses (Bourne et al., 1974; Mosenden and Tasken, 2011) and plays a role in the suppressive activity of T cells (Bopp et al., 2007). To analyze a possible role for coronin 1 in the modulation of cAMP signaling in T cells, membranes from WT and *Coro1a*$^{-/-}$ T cells were stimulated with forskolin and cAMP levels were determined. Depletion of coronin 1 resulted in significantly reduced production of cAMP (Figure S5C,D). However, when intracellular

concentrations of cAMP were determined, *Coro1a*$^{-/-}$ T cells showed enhanced levels of cAMP relative to WT T cells (Figure 4A,B). The fact that activation or inhibition of components of the cAMP pathway is known to result in compensatory modulation of other proteins in this pathway (Erdogan and Houslay, 1997; Krumins and Gilman, 2006), prompted us to analyze levels of the cAMP degrading phosphodiesterase 4 (PDE4), a key regulator of cAMP in T cells (Erdogan and Houslay, 1997; Giembycz et al., 1996; Omori and Kotera, 2007). PDE4 protein amounts were severely reduced in T cells lacking coronin 1 (Figure 4C, S5E). Consistent with reduced PDE4, stimulation of T cells with the adenylate cyclase activator forskolin resulted in elevated cAMP concentrations in T cells lacking coronin 1 (Figure 4D). The inclusion of the PDE4 inhibitor rolipram, which enhanced the fold induction of cAMP in WT T cells, did not do so in *Coro1a*$^{-/-}$ T cells upon stimulation (Figure 4E). This suggests that the absence of coronin 1 resulted in elevated cAMP levels as a result of a compensatory decrease in PDE4 protein in T cells. Analysis of migrated healthy naïve T cells as well as memory T cells (Mueller et al., 2011) revealed elevated cAMP concentrations in all *Coro1a*$^{-/-}$ T cell subsets (Figure 4F,G). Also, human T cells (Jurkat) lacking coronin 1 through CRISPR-Cas9-mediated deletion of the *Coro1a* gene showed a similar reduction of PDE4 protein as well as enhanced cAMP concentration (Figure 4H-J), confirming that the role of coronin 1 in regulating cAMP-PDE4 levels is T cell intrinsic. Coronin 1-mediated cAMP modulation was furthermore found to occur in primary human immune cells, as peripheral blood mononuclear cells (PBMC) from a human subject harboring a destabilizing V134M mutation in coronin 1 (Jayachandran et al., 2014; Moshous et al., 2013) showed reduction of PDE4 protein and increased cAMP concentration (Figure 4K-N). Thus,

our findings suggest a critical role for coronin 1 in maintaining the levels of cAMP in both mouse and human T cells in a cell-intrinsic manner.

To further delineate coronin 1-dependent regulation of cAMP signaling in T cells, we analyzed the activity as well as localization of protein kinase A (PKA), a serine/threonine kinase whose regulatory subunits bind cAMP (Taylor et al., 2005). Consistent with increased cAMP levels in the absence of coronin 1, lysates from *Coro1a*$^{-/-}$ T cells showed elevated levels of PKA activity (Figure 5A), and the catalytic subunit of PKA (PKAc) was translocated to the nucleus in the absence of coronin 1 (Figure S5F). In T cells, increases in cAMP levels inhibit the activation of CalModulin Kinase IV (CaMKIV) by blocking its phosphorylation at Thr-196 (Soderling, 1999; Wayman et al., 1997). Consistent with elevated PKA activity in *Coro1a*$^{-/-}$ T cells, CaMKIV (T^{196}) phosphorylation was reduced (Figure 5B). CaMKIV is one of the prime kinases needed for the activation of the cAMP Response Element Binding (CREB) protein in T cells (Anderson and Means, 2002; Anderson et al., 1997), and phosphorylation of CREB (S^{133}) was impeded in the absence of coronin 1 (Figure 5C-E). To address the role for PKA and CaMKIV in the phosphorylation of CREB in unstimulated T cells *in vivo*, freshly isolated cells were immediately incubated with or without inhibitors for PKA or CaMKIV. Blocking PKA (with H89) in *Coro1a*$^{-/-}$ T cells resulted in an increase in CREB phosphorylation, whereas blocking CaMKIV with KN93 further reduced the pCREB status (Figure 5F). While inhibition of PKA did not affect proliferation of WT T cells, it significantly enhanced the proliferation of *Coro1a*$^{-/-}$ T cells (Figure 5G).

To analyze whether modulation of cAMP could alter T cell numbers *in vivo*, we manipulated cAMP levels through administration of the phosphodiesterase inhibitor rolipram in WT mice (elevating cAMP) or treated *Coro1a*$^{-/-}$ mice with the PKA inhibitor H89 (reducing cAMP). Administration of rolipram in WT mice significantly reduced naïve T cell numbers (Figure 5H) whereas administration of H89 to inhibit cAMP-PKA signaling in *Coro1a*$^{-/-}$ T cells resulted in a significant increase in naïve T cell numbers (Figure 5I).

Selective suppression of allo- but not anti-microbial T cell responses by cAMP—Role of CD80-mediated CD28 activation

Next, we asked if the elevated cAMP differentially affected T cell responses against allo-antigens versus infectious antigens. We compared the effect of rolipram on T cell proliferative responses induced either by MHC-mismatched antigen presenting cells (APCs) or MHC-matched APCs incubated with *Salmonella* to load the APC's with antigens of microbial origin. Whereas rolipram depressed T cell proliferative responses against allo-antigens, proliferation against infectious antigens were not significantly affected (Figure 6A,B). The selectivity of cAMP-mediated suppression of alloresponses versus anti-microbial T cell activation was associated with differential induction of MHC class II and the co-stimulatory molecules CD80 and CD86 on APCs (Figure 6C and S6A,B). Elevated costimulatory induction was also observed *in vivo* following microbial antigen relative to alloantigen stimulation (Figure S6C,D). Blocking CD80-mediated co-stimulation using blocking antibodies, either alone or together with CD86, prevented anti-infectious responses even in the presence of rolipram, suggesting a role for CD80-mediated T cell activation in overcoming cAMP

mediated immunosuppression (Figure 6D and S6D). Exclusion of CD28 co-stimulation in the context of TCR triggering (Figure 6E) rendered T cells vulnerable to inhibition of proliferation by rolipram (IC50 of~ 20 μM for CD3 stimulus versus >320 μM for CD3-28 stimuli), suggesting the ability of CD80-CD28 signaling to overcome the cAMP-mediated inhibition of immune responses during microbial infections. *Coro1a*$^{-/-}$ antigen presenting cells were equally capable of triggering allogeneic T cells to proliferate (Figure S6F). These results show the potential for elevating cAMP levels inside T cells through coronin 1 depletion to selectively block alloresponses while maintaining anti-infectious responses.

Coro1a$^{-/-}$ *CD4*$^{+}$ *CD25*$^{-}$*Tconv cells induce tolerance against alloreactive T cells*

The specific suppression of alloreactivity, without compromising immunity against microbial pathogens, led us to explore whether *Coro1a*$^{-/-}$ T cells were able to induce tolerance against allografts. *Rag2*$^{-/-}$ mice carrying minor mismatched allografts were adoptively transferred with *Coro1a*$^{-/-}$CD4^{+}CD25^{-} T cells (Figure 7A and Figure S7A), followed by a challenge with WT CD4^{+} T cells (Figure 7B). The prior transfer of *Coro1a*$^{-/-}$ T cells conferred protection against a subsequent challenge with WT CD4^{+} T cells (Figure 7B). Control experiments revealed both the presence as well as the functionality of the transferred WT T cells (Figure 7A, 7B, and S7B). Moreover, the prior transfer of *Coro1a*$^{-/-}$ T cells filling up the available niche in peripheral lymphoid organs was unlikely to be the reason for the failure of WT T cells to reject the graft as the number of *Coro1a*$^{-/-}$ T cells in these animals were many fold less compared with only WT T cell transfer (data not shown).

To analyze a potential for pharmacological manipulation of this pathway to modulate graft rejection, cAMP levels were manipulated *in vivo* through administration of the PDE inhibitor rolipram in mice bearing a major MHC mismatched skin allograft (BM12 I-A^{bm12}). Administration of rolipram resulted in significantly prolonged survival of allografts in comparison to vehicle only-treated control (Figure 7C). Administration of the PKA inhibitor H89 *in vivo* in *Coro1a*$^{-/-}$ mice bearing a major MHC-mismatched allograft that have been adoptively transferred with wild-type CD4 T cells reversed the allograft tolerance (Figure 7D). These results suggest that modulation of the coronin 1-dependent axis may be beneficial in the prevention of allograft rejection.

Discussion

One of the most problematic consequences of immunosuppression following allograft transplantation is the association with a high susceptibility towards pathogenic and opportunistic infections (Avery, 2013; Birkeland et al., 2000). Mechanisms allowing a selective suppression of allo-reactive T cells while avoiding suppression of pathogen-specific immune cell responses are currently unknown. Here, we show that deletion in mice of the gene coding for coronin 1, an essential regulator of peripheral naïve T cells, results in tolerance towards allografts while maintaining robust immune responses against a range of pathogenic microbes as well as an absence of immunosuppression-mediated pathology.

We further show that the here described tolerance towards allografts is linked

towards a role for coronin 1 in modulating the CaMKIV-pCREB pathway, and that the absence of coronin 1 in T cells resulted in upregulation of cAMP and increased activity of PKA, thereby blocking CaMKIV and resulting in reduced CREB phosphorylation.

The elevated levels of cAMP are likely to be a result of adaptive changes in T cells induced by the absence of coronin 1, that is known to modulate cAMP responses following cell surface stimulation (Jayachandran et al., 2014; Suo et al., 2014). Indeed, deletion and/or inhibition of components of the cAMP-PKA pathway modulate levels of other proteins that play a role in this pathway (Dupre et al., 2009; Erdogan and Houslay, 1997; Krumins and Gilman, 2006). In particular, we found that *Coro1a*$^{-/-}$ T cells expressed reduced amounts of the cAMP degrading enzyme PDE4, a central regulator of cAMP in T cells (Arumugham and Baldari, 2017). Furthermore, a PDE4 inhibitor, rolipram, phenocopied the coronin 1 depletion in an allograft rejection model. Conversely, *in vivo* PKA inhibition in *Coro1a*$^{-/-}$ mice reversed the observed allograft tolerance.

Several lines of evidence argue for induction of tolerance to be responsible for the observed long-term retention of the allografts upon coronin 1 ablation, rather than a paucity of T cells: first, adoptive transfer of large numbers of *Coro1a*$^{-/-}$ CD4^{+} T cells failed to induce rejection. Second, *Coro1a*$^{-/-}$-deficient T cells displayed markers associated with an immunosuppressive phenotype, and third, conventional (CD4^{+}CD25^{-}) *Coro1a*$^{-/-}$ T cells were able to prevent wild type CD4^{+} T cells from allograft rejection upon a challenge with adoptive transfer of alloreactive T cells *in viv*o.

The paucity of peripheral naïve T cells in the absence of coronin 1 in mice did not result in a predisposition towards infections. This suggests that a minimal number of naïve T cells may be sufficient to effectively control these pathogens, including the generation of specific T cell responses, although coronin 1 may be required to contain infections where the timing (Tchang et al., 2013) or rapid clearance of pathogens at specific niches is crucial as seen following MCMV infection. Although *Coro1a*$^{-/-}$ individuals have been reported to display an enhanced susceptibility towards infections, in most of these cases additional genetic aberrations are present, such as those in genes involved in the regulation of immune function (NLRP7, STAT2, NCF2, APOB48R (Punwani et al., 2015; Shiow et al., 2009; Stray-Pedersen et al., 2014; Yee et al., 2016). Whether or not in human, as opposed to mice, coronin 1 loss-of-function is associated with infectious complications such as susceptibility to certain viruses (Moshous et al., 2013; Stray-Pedersen et al., 2014) or whether additional confounding factors are responsible for the observed susceptibility remains to be analyzed.

The exact role for cAMP in promoting immunosuppression remains to be elucidated. cAMP is known as a negative regulator of T cell activation (Bourne et al., 1974; Wehbi and Tasken, 2016), and immunosuppressive activities of cAMP have predominantly been ascribed to its capacity to block proximal TCR signaling (Vang et al., 2001; Wehbi and Tasken, 2016). However, proximal TCR signalling appears to be unaltered in the absence of coronin 1 (Mueller et al., 2008), which is also consistent with normal T cell selection in the thymus (Lang et al., 2017; Mueller et al., 2008) as well as the here described normal T cell

responses against microbial pathogens. While *Coro1a*$^{-/-}$ T cells were also reported to be defective in the activation of the calcineurin signaling pathway (Mueller et al., 2011; Mueller et al., 2008), this cannot explain the suppression of WT T cells from allograft rejection by *Coro1a*$^{-/-}$ T cells as described here.

The immunosuppressive activities of cAMP have also been implicated in the function of FoxP3- and CD25-positive Treg cells (Josefowicz et al., 2012; Sakaguchi et al., 2008; Tang and Bluestone, 2013). However, multiple lines of evidence suggest that the immunosuppression observed in the absence of coronin 1 is not due to Treg cells: first, depletion of CD25^{+} cells failed to interfere with the immunosuppression induced by *Coro1a*$^{-/-}$ T cells; second, *Coro1a*$^{-/-}$ conventional CD4^{+} T cells did not express markers that define Treg cells. Third, whole transcriptome analysis of conventional *Coro1a*$^{-/-}$ T cells showed these to carry a distinct T cell signature.

Coro1a$^{-/-}$ T cells were able to inhibit the proliferation of WT T cells *in vivo*, as evidenced first by reduction of WT T cell proliferation in vivo, and second by the ability of a prior transfer of *Coro1a*$^{-/-}$ T cells to suppress alloreactive T cells. Such suppression by *Coro1a*$^{-/-}$ T cells may involve direct contact between *Coro1a*$^{-/-}$ and WT T cells; however, our attempts to asses a direct contact using an *in vivo* transfer assay (Bodor et al., 2012) were unsuccessful. Possibly, activation of the cAMP-PKA pathway upon coronin 1 deletion induces the release of molecules in an autocrine or paracrine manner or *in trans* as evidenced by the upregulation of immunosuppressive markers. Such a scenario would be consistent with the here shown capacity of *Coro1a*$^{-/-}$ T cells to suppress WT T cells *in vivo.*

While T cell responses towards allografts are suppressed, immunity against pathogenic microbes was unperturbed in the absence of coronin 1. This was found to be due to the ability of CD28-dependent co-stimulation through CD80, but not CD86, to overcome cAMP-mediated suppression following microbial infection. Interestingly, CD80 and CD86 activate distinct signaling pathways, and although the exact roles of CD80 and CD86 activation of CD28 during allograft immune responses remain unclear (Ford, 2016; Zheng et al., 1997), the data presented here provide support for a role of CD80 in T cell activation towards microbial antigens, even in the presence of the immunosuppressive molecule cAMP.

The here defined role for coronin 1 in the induction of a tolerogenic environment while maintaining immunity against microbial pathogens opens an interesting perspective for developing immunosuppressive strategies. Current regimen employed to prevent graft rejection largely depend on the use of calcineurin blockers. Given the ubiquitous expression of calcineurin and its importance in diverse physiological processes, calcineurin inhibitors are associated with severe side effects including infections and malignancies. Furthermore, recent work exploring modulation of co-stimulatory and co-inhibitory pathways lead to the realization that such approaches may also perturb Treg cell homeostasis, with enhanced rejection and the potential to develop autoimmunity (Ford, 2016; Schmidt et al., 2009). In contrast, depletion of coronin 1, at least in mice, did not result in any immunomodulatory phenotype besides the demonstrated tolerance towards allografts. The predominant expression of coronin 1 in leukocytes and

the observation in both mice and human that its deletion appears to exclusively affect naïve T cells suggests that compounds targeting coronin 1 or the coronin 1-dependent cAMP pathway may allow effective graft tolerance without overt immunosuppression. Additionally, with the advent of technologies to edit genomes in hematopoietic stem cells, one might consider targeting coronin 1 to promote a tolerogenic milieu in transplant recipients.

Figure Legends

Figure 1: Mice lacking coronin 1 are tolerant toward cardiac and skin allografts

(A) C57BL/6 WT or *Coro1a*$^{-/-}$ mice (I-A^{b}) recipients were subjected to heterotopic cardiac transplantation using BALB/c (I-A^{d}) donors. Shown is the percent survival of the graft. n=9 WT and 8 *Coro1a*$^{-/-}$ mice. Results are combined from two independent experiments.

(B,C) Cardiac grafts from WT or *Coro1a*$^{-/-}$ recipients were assessed by hematoxylin-eosin (H/E) and Van Gieson's staining at the time of rejection (in WT recipients, B) or at the time of study termination (day 106, C), in *Coro1a*$^{-/-}$ recipients.

(D) Representative image of a major mismatched skin graft (BM12 skin grafts, I-A^{bm12}) onto either a WT (day 10) or *Coro1a*$^{-/-}$ recipient (I-A^{b}; day 14).

(E) Survival of major mismatched skin graft (BM12 skin grafts, I-A^{bm12}) transplanted onto C57BL/6 WT or *Coro1a*$^{-/-}$ recipients (I-A^{b}). A representative of three independent experiments is shown.

(F) Major mismatched skin grafts (BM12 skin grafts, I-A^{bm12}) transplanted onto WT or *Coro1a*$^{-/-}$ recipients (I-A^{b}) were assessed by H/E staining at the time of rejection in WT recipients. Scale bar = 1 μm (upper panels), scale bar= 50 μm (lower panels).

(G) Survival of minor mismatched skin grafts (BALB/c (I-A^{d}), transplanted onto WT or *Coro1a*$^{-/-}$ recipients. n= 10 mice per genotype. E,G: A representative of three independent experiments is shown.

See also Figure S1.

Figure 2: Coro1a$^{-/-}$ mice maintain pathogen-specific immune responses

(A,B) Mice were infected with *S. aureus* (A) or *C. albicans* (B) subcutaneously, sacrificed and CFU enumerated from the sites indicated. n= 8-10 mice/genotype. From two independent experiments. No statistical difference, Mann-Whitney *U*-test.

(C) WT or *Coro1a*$^{-/-}$ mice were infected orally with *S. typhimurium*, sacrificed when moribund and the bacteria enumerated from spleen and liver. n=15 mice/genotype. No statistical difference, Mann-Whitney *U*-test.

(D) *Left panel:* WT or *Coro1a*$^{-/-}$ mice were adoptively transferred with Cell Trace Violet-labelled OTII CD4^{+} T cells from corresponding genotypes followed by infection with normal *Salmonella* or OVA-expressing *Salmonella*. Proliferation of adoptively transferred cells was assessed at day 7. n = 5 mice/ group (representative of two independent experiments is shown). SEM, Students *t*-test. *Right panel:* Enumeration of CFUs from indicated organs. No statistical significance. Unpaired *t*-test.

(E) WT or *Coro1a*$^{-/-}$ mice were either left unvaccinated or vaccinated with avirulent *Salmonella* and challenged six weeks later with virulent *Salmonella* followed by CFU enumeration (spleen and liver) on D5. n = 5 mice group for unvaccinated mice and 6-9 for the vaccinated group. *Coro1a*$^{-/-}$ mice had significantly lower *Salmonella* burden. $p<0.05$ for unvaccinated, $p<0.01$ for vaccinated groups from liver between WT and *Coro1a*$^{-/-}$ mice. Lines represents mean and Unpaired *t*-test.

(F,G) Kinetics of MCMV clearance (F) and T cell responses against MCMV antigens (G) in WT and *Coro1a*$^{-/-}$ mice. P values (*** p<0.001; * p<0.05) were calculated by using the two-tailed Mann-Whitney *U*-test.; DL: Detection limit. A-F: Each symbol represents data from one mouse; horizontal lines represent the mean of each group.

See also Figure S2.

Figure 3: Coro1a-deficiency induces allo-tolerance in a Treg cell-independent manner

(A) Survival of minor BALB/c (I-A^{d}) antigen-mismatched skin grafts transplanted onto *Coro1a*$^{-/-}$ (Cor 1$^{-/-}$) mice followed by adoptive transfer (AT, arrow) of WT (10^{6}) CD4^{+} T cells. RAG2$^{-/-}$ mice bearing allografts transferred with 20'000 WT CD4^{+} T cells (black dotted line) serve as rejection control. Blue trace: WT mice transplanted with minor antigen-mismatched grafts (control). n=5 mice for minor-WT group and minor-RAG2$^{-/-}$ group. n=7 mice for 10^{6} WT CD4^{+} T cell transferred group. *Inset:* Enumeration of transferred WT CD4^{+} T cells from spleen, lymph nodes and blood by flow cytometry at study termination shown in Figure 3A.

(B) Survival of major mismatched skin grafts (BM12 skin grafts, I-A^{bm12}) transplanted onto *Coro1a*$^{-/-}$ mice (I-A^{b}) followed by adoptive transfer (arrow) of WT (5 x 10^{6}) CD4^{+} T cells. At the time of transfer, as a control, 20'000 WT CD4^{+} T cells were transferred into RAG2$^{-/-}$ mice bearing allografts (gray trace: rejection control). Blue trace: WT mice transplanted with BM12 grafts (control). **** P<0.0001. Log-rank test between RAG2$^{-/-}$ and *Coro1a*$^{-/-}$ mice receiving WT CD4^{+}

cells. Representative of three independent experiments. n=4 mice for major->WT group, 5 for major->RAG2$^{-/-}$ group, n= 6 mice for 5 x 10^6 CD4$^+$ group. *Inset:* Enumeration of transferred WT CD4$^+$ T cells as explained in A.

(C) Survival of minor BALB/c (I-A^d) antigen-mismatched skin grafts transplanted onto *Coro1a*$^{-/-}$ recipients that were either untreated or depleted of CD25$^+$ cells by administration of PC61 (see arrow) at the time when all WT recipients had completely rejected the graft. n=5 mice for minor-> WT group and 4 mice for minor-> Cor 1$^{-/-}$ group. n=7 mice for PC61 administered group. Note: The traces from both the *Coro1a*$^{-/-}$ groups overlap.

(D) Survival of minor antigen-mismatched skin grafts transplanted onto *Coro1a*$^{-/-}$ recipients post PC61 administration and adoptive transfer (i.v.) of the indicated numbers of WT CD4$^+$ T cells. RAG2$^{-/-}$ mice bearing skin grafts and receiving WT CD4$^+$ T cells and as well injected with PC61 mAb serve as a control for adoptive transfer and vitality of transferred cells. **** P<0.0001. Log-rank test between RAG2$^{-/-}$ and *Coro1a*$^{-/-}$ mice receiving WT CD4$^+$ cells. n=7 mice for minor-> Cor 1$^{-/-}$ with PC61 administered group, n= 5 mice for minor-> Cor 1$^{-/-}$ with WT CD4$^+$ T cells and n=10 mice for RAG2$^{-/-}$ with WT CD4$^+$ T cells and PC61 injected group. Note: The traces from the *Coro1a*$^{-/-}$ groups overlap.

(E) Principal component analysis of transcriptomes from biological triplicates of conventional (CD4$^+$CD25$^-$) and regulatory T cells (CD4$^+$CD25$^+$) between WT (WT) and *Coro1a*$^{-/-}$ (KO) T cells. Principal components were calculated in R using the prcomp function.

(F-H): *In vivo* suppression. F: WT (Ly5.1) CD4$^+$CD25$^-$ cells (10^6) were either injected alone or with equal numbers of *Coro1a*$^{-/-}$ (Ly5.2) CD4$^+$CD25$^-$ cells into RAG2$^{-/-}$ mice. Mice were sacrificed two weeks later and the transferred cells

quantified by flow cytometry. The plot shows number of $Ly5.1^+$ cells recovered from spleen and lymph nodes (axillary, brachial and inguinal). n= 5 mice/group, representative of three independent experiments. * P<0.05. Unpaired Student's *t*-test. G, H: CFSE labelled WT (Ly5.1) $CD4^+CD25^-$ cells (0.5×10^6) were either injected alone or with equal numbers of WT (Ly5.2) $CD4^+CD25^-CD62L^{Hi}$ or *Coro1a*$^{-/-}$ (Ly5.2) $CD4^+CD25^-$ cells into $RAG2^{-/-}$ mice. Mice were sacrificed one week later and the transferred Ly5.1 cells assessed for CFSE dilution by flow cytometry from peripheral lymph nodes. In G, percentage of cells that were CFSE high are shown. In H, representative CFSE dilution profiles are shown. n= 4 mice for Ly5.1 and Ly5.1 + Cor $1^{-/-}$ Ly5.2 groups and 3 for Ly5.1 + WT Ly5.2 mice group. Representative of two independent experiments. SEM shown and * P<0.05, **P<0.01. Unpaired Student's *t*-test.

See also Figure S3 and S4.

Figure 4: Coronin 1 modulates cAMP in mouse and human T cells

(A) cAMP levels of WT or *Coro1a*$^{-/-}$ splenic T cells assessed immediately (HTRF assay). SEM from five independent experiments. *** P<0.001. Unpaired Student's *t*-test.

(B) WT and *Coro1a*$^{-/-}$ splenic T cells were mixed (1:1) and immuno-stained for cAMP, coronin 1 and nuclei and imaged using a confocal microscope. Bar = 8 μm. Two independent experiments.

(C) Equal amounts of WT or *Coro1a*$^{-/-}$ splenic T cell lysates were immunoblotted for the indicated antigens. Representative of five independent experiments.

(D) cAMP levels of either WT or *Coro1a*$^{-/-}$ splenic T cells stimulated with 100 μM forskolin for 10 min at 37°C without the addition of rolipram. Error bars represent standard error from five independent experiments. ** P<0.01. Unpaired Student's *t*-test.

(E) Splenic T cells from WT or *Coro1a*$^{-/-}$ animals were pretreated with DMSO or 100 μM rolipram (30 min, 37°C, 5% CO_2), and stimulated with 100 μM forskolin (FSK, 10 min, 37°C) and cAMP production assessed. Shown is the fold induction of cAMP production of cells stimulated with forskolin in the presence of rolipram compared to cells stimulated in the absence of rolipram. Values represent SEM calculated from four independent experiments. ** P<0.01, *** P<0.001. Unpaired Student's *t*-test.

(F,G) cAMP levels of migrated WT or *Coro1a*$^{-/-}$ naïve (G) or memory (H) T cells stimulated with either 10 μM isoproterenol (Iso) or 100 μM of FSK (10 min, 37°C). The values for the unstimulated cells were outside the dynamic range. Two independent experiments. ** P<0.01. Unpaired Student's *t*-test. Right panels: Apoptotic status of migrated cells by Annexin V staining. Top: WT and bottom: *Coro1a*$^{-/-}$ panel.

(H) Immunofluorescence analysis of coronin 1 in WT and *Coro1a*$^{-/-}$ Jurkat T cells by using an α-coronin 1 antibody, followed by staining with Alexa-Fluor 568 conjugated secondary antibody. Nuclei were stained using DRAQ5. Bar =10μm. Three independent experiments.

(I) WT or *Coro1a*$^{-/-}$ Jurkat cells were lysed and equal protein amounts immunoblotted for PDE4 followed by reprobing with α-coronin 1 and α-actin antibodies. Representative blot from three independent experiments.

(J) cAMP levels of either WT or *Coro1a*$^{-/-}$ Jurkat cells. Cells were serum starved for 2 h and stimulated with 100 μM FSK (10', 37°C). Representative result out of at least three independent experiments.

(K) Immunoblotting of PBMC lysates from control donors (Ctrls) and a *Coro1a*$^{-/-}$ subject (V134M) using coronin 1, PDE4 and GAPDH antibodies.

(L) cAMP levels assayed from healthy (control) or *Coro1a*$^{-/-}$ V134M PBMCs are shown. cAMP levels were assessed from the lysates without stimulation or addition of PDE4 inhibitor rolipram. P values (**** p<0.0001), unpaired Student's *t*-test.

(M) Analysis of cAMP levels by immunofluorescence of control donors versus a *Coro1a*$^{-/-}$ individual (V134M, hypomorphic mutation) stained for cAMP (AF488), coronin 1 (AF568) and DRAQ5. n=two independent experiments. Bar= 10 μm.

(N) Quantitation of cAMP fluorescence intensity from the images using image J software. n=430 cells for control donors and 168 cells for the *Coro1a*$^{-/-}$ individual (V134M). P values (**** p<0.0001), unpaired Student's *t*-test. Two independent experiments.

See also Figure S5.

Figure 5: Coro1a*$^{-/-}$ *deficiency modulates the CaMKIV/pCREB pathway in T cells

(A) Protein kinase A (PKA) activity analyzed from equal amounts of splenic T cell lysates from WT or *Coro1a*$^{-/-}$ mice using a PKA specific substrate. n=3 independent experiments. Unpaired Student's *t*-test. * P=<0.05.

(B) Equal amounts of splenic T cell lysates from WT or *Coro1a*$^{-/-}$ mice were immunoblotted for phospho-CaMKIV (Thr^{196} pCaMKIV), actin and coronin 1. Representative blot from three independent experiments.

(C) Equal amounts of splenic T cell lysates from WT or *Coro1a*$^{-/-}$ mice were immunoblotted for phosphoCREB (S^{133} pCREB), total CREB, actin and coronin 1. Representative blot from four independent experiments.

(D,E) T cells from WT and *Coro1a*$^{-/-}$ spleens were mixed in a 1:1 ratio on a coverslip and stained for pCREB (AF488), coronin 1 (AF568) and DRAQ5 and imaged by confocal microscopy. Bar = 8 μm. Three independent experiments. P values (*** $p<0.001$), unpaired Student's *t*-test.

(F) Equal amounts of lysates from *Coro1a*$^{-/-}$ splenic T cells subjected to incubation with PKA inhibitor (H89, 1μM) or CaMKIV inhibitor (KN93, 10 μM) and immunoblotted for phosphoCREB (S^{133} pCREB), total CREB and actin. At least three independent experiments.

(G) Splenic T cells isolated from WT or *Coro1a*$^{-/-}$ mice were stimulated (α-CD3/28 antibodies) and incubated with PKA inhibitor (H89, 1μM) or CaMKIV inhibitor (KN93, 10 μM) and assessed for proliferation by incorporation of tritiated thymidine. The values are depicted as percentages relative to the proliferation observed with vehicle (DMSO) controls. Three independent experiments. P values (*** $p<0.001$), unpaired Student's *t*-test.

(H) Top panel: WT C57BL/6 mice were treated either with rolipram (5 mg/kg body weight SC, twice daily) or the control vehicle for a duration of 7 days and assessed for naïve (CD4^{+} CD62L^{hi} CD44^{low}) and effector memory CD4^{+} T cells (CD4^{+} CD62L^{hi} CD44^{low}) in tail blood by flow cytometry. P values (** $p<0.01$) were calculated using unpaired Student's *t*-test. Three independent experiments.

Bottom panel: Enumeration of naïve ($CD8^+$ $CD62L^{hi}$ $CD44^{low}$) and effector memory $CD8^+$ T cells ($CD8^+$ $CD62L^{hi}$ $CD44^{low}$). P values (** $p<0.01$ and *** $p<0.001$) were calculated using unpaired Student's *t*-test. n= 5 mice per group. Three independent experiments.

(I) Top panel: *Coro1a*$^{-/-}$ C57BL/6 mice were treated either with H89 (40 mg/kg body weight SC, twice daily) or the control vehicle for a duration of 4 days and assessed for naïve ($CD4^+$ $CD62L^{hi}$ $CD44^{low}$) and effector memory T cells $CD4^+$ T cells ($CD4^+$ $CD62L^{hi}$ $CD44^{low}$) in tail blood by flow cytometry. P values (* $p<0.05$) were calculated using unpaired Student's *t*-test. n= 4 mice per group. Three independent experiments. Bottom panel: Enumeration of naïve ($CD8^+$ $CD62L^{hi}$ $CD44^{low}$) and effector memory $CD8^+$ T cells ($CD8^+$ $CD62L^{hi}$ $CD44^{low}$) as analyzed in (H). P values (* $p<0.05$) were calculated using unpaired Student's *t*-test. n= 4 mice per group. Three independent experiments.

Figure 6: Selective suppression of allo-response but not anti-infectious T cell responses by cAMP: Role of CD80-mediated CD28 activation.

(A) *T cell responses to allogeneic stimuli (MLR)*: APC (Balb/c ($I\text{-}A^d$)) induced WT CD4 T cell (C57BL/6 ($I\text{-}A^b$)) proliferation in the presence of DMSO *(left panel)* or 10μM rolipram *(middle panel)*. *Right panel:* Percentages of WT CD4 T cells that have proliferated (CTV low) in the presence of 10μM rolipram and DMSO. Values are derived from triplicate samples. Representative of two independent experiments. *** $P<0.001$. Unpaired Student's *t*-test.

(B) *T cell responses to infectious stimuli*: Analysis of WT OTII CD4 T cell (Ly5.2 C57BL/6 ($I\text{-}A^b$)) proliferation by CTV dye dilution upon co-incubation with APCs (Ly5.1 C57BL/6 ($I\text{-}A^b$)) that had been infected with Ova-*Salmonella* in the

presence of DMSO *(left panel)* or 10μM rolipram *(middle panel)*. *Right panel:* Percentages of WT OTII CD4 T cells that have proliferated (CTV low) in the presence of 10 μM rolipram and DMSO. Values are derived from triplicate samples. Three independent experiments. No statistical significance.

(C) APCs isolated from spleens of Balb/c (I-A^d) and C57BL/6 (I-A^b) mice were either left uninfected or infected with Ova-*Salmonella* and analyzed 24h later by flow cytometry for $MHCII^{hi}CD80^{hi}$ and $MHCII^{hi}CD86^{hi}$ status. The data shown are from the CD11c gated population. ** P<0.01, **** P<0.0001. Unpaired Student's *t*-test. Representative of three independent experiments.

(D) Analysis of WT OTII CD4 T cell (C57BL/6 (I-A^b)) proliferation upon co-incubation with APCs (C57BL/6 (I-A^b)) that had been infected with Ova-*Salmonella* in the presence of the indicated antibodies and rolipram (10 μM). Shown are the percentage of cells that are CTV low from triplicate samples. **** P<0.0001. Unpaired Student's *t*-test.

(E) Analysis of WT CD4 T cell (C57BL/6) proliferation upon stimulation with plate-bound α-CD3 either with or without soluble α-CD28 in the presence of indicated amounts of rolipram for 3.5 days. Shown are the percentages of CD4 T cells that are CTV low. *Left panel;* α-CD3 and α-CD28 stimuli. Right panel; only α-CD3 stimulus. Representative of two independent experiments.

See also Figure S6.

Figure 7: Induction of tolerance against alloreactive T cells by Coro1a$^{-/-}$ CD4$^+$ CD25$^-$ Tconv cells and pharmacological modulation of cAMP in vivo

(A) RAG2$^{-/-}$ mice were transplanted with a minor histocompatibility antigen-mismatched graft (BALB/c (I-A^{d})) followed by adoptive transfer of either *Coro1a*$^{-/-}$ CD4^{+}CD25^{-} T cells (Tconv, red trace), WT CD4+ T cells (rejection control, blue trace) or left untransferred (negative controls, Grey trace). Note: The traces from the *Coro1a*$^{-/-}$ and untransferred groups overlap. ** P<0.01, Log-rank test between *Coro1a*$^{-/-}$ and WT T cell transferred group.

(B) RAG2$^{-/-}$ mice that were previously transferred with *Coro1a*–deficient Tconv cells (from panel A, and had not rejected the allografts), were challenged on day 60 by adoptive transfer of WT CD4^{+} T cells (green trace) or left untreated (red trace) and kinetics of rejection monitored. RAG2$^{-/-}$ mice carrying a minor histocompatibility antigen-mismatched allograft and not having received *Coro1a*$^{-/-}$ T cells but were transferred with WT CD4^{+} T cells served as controls for adoptive transfer and vitality of transferred cells (Rejection control, gray traces). ** P<0.01. Log-rank test between WT challenge and only WT T cell transferred RAG2$^{-/-}$ group. n=4 mice for untransferred group. n=3 for *Coro1a*$^{-/-}$ CD4^{+}CD25^{-} T cell transferred group. n= 4 mice for WT CD4^{+} T cells shown in panel A, n= 8 mice for WT CD4^{+} T cells, n= 7 mice for *Coro1a*$^{-/-}$ CD4^{+}CD25^{-} T cell (200'000) transfer followed by challenge with WT CD4^{+} T cells group. Note: The traces from the *Coro1a*$^{-/-}$ groups overlap.

(C) WT C57BL/6 mice carrying a major MHC mismatched skin allograft (BM12 skin grafts, I-A^{bm12}) were treated either with rolipram or the control vehicle and monitored for kinetics of allograft rejection. P values (** p<0.001) were calculated using Mantel-Cox log-rank test. n= 8 mice for rolipram treated group. n= 4 mice per group for untreated and DMSO treated group.

(D) Survival of BM12 RAG2$^{-/-}$ skin grafts in *Coro1a*$^{-/-}$ recipients after transfer of WT C57BL/6 with application of either DMSO or the PKA inhibitor H89. Following transplantation, the recipient mice were adoptively transferred with CD4^{+} T cells i.v. on day 0 day. H89 application (40 mg/kg body weight) was initiated a day prior to the day of adoptive transfer. n=3 mice for DMSO group, 4 mice for H89 group, n=3 mice for rejection control RAG2$^{-/-}$ with WT CD4 AT group. p=0.07, Log-Rank test between DMSO and H89 group.

See also Figure S7.

STAR Methods

Contact for Reagent and Resource Sharing

Further information and requests for resources and reagents should be directed to and will be fulfilled by the Lead Contact, Jean Pieters (jean.pieters@unibas.ch).

Experimental Model and Subject Details

Cells

Jurkat cells (ATCC, TIB-152) were grown in RPMI-1640 (Sigma) containing penicillin/streptomycin (Gibco), 2 mM L-glutamine (Gibco) and 10% FCS (PAA). Cells were incubated in a 37° C humidified incubator with a 5% CO_2.

Mice

Coro1a$^{-/-}$ (available from The Jackson Laboratory (JAX stock no. 030203)) and WT C57BL/6 mice were described before (Jayachandran et al., 2007) and were used from backcross 8 or backcross 10 to C57/BL6. All cohorts were age (8-16 weeks) and sex matched and both males and females used for the studies. RAG2$^{-/-}$ (Shinkai et al., 1992) and H2-bm12 (I-A^{bm12}, McKenzie et al., 1979) mice were obtained from Prof. Ed Palmer (Basel, Switzerland). Minor histocompatibility antigen-mismatched mice ('minor' in short) were generated in house by backcrossing four times the F1 (C57BL/6 x BALB/c) progeny to the C57BL/6 parental line. This minor histocompatibility antigen-mismatched donor mouse line was validated for expression of BALB/c and C57BL/6 MHC antigens by flow cytometry that confirmed expression of C57BL/6 MHC molecules and none of the BALB/c MHC molecules (Figure S1). Furthermore, a 1450 single-nucleotide

polymorphism (SNP) analysis showed this strain to possess 96.9% of C57BL/6 genome with the rest coming from BALB/c genome (data not shown). OTII transgenic mice (C57BL/6; B6-Tg(TCRαTCRβ)425Cbn/J)) were obtained from the Swiss Immunological Mouse Repository (SwimR) and crossed with *Coro1a*$^{-/-}$ mice. OTII x *Coro1a*$^{-/-}$ transgenics were backcrossed at least 4 times to parental lines (Barnden et al., 1998). All animal experimentation was approved by the veterinary office of the Canton of Basel-Stadt (approved license number 1893 and 2326) and performed according to local guidelines (Tierschutz-Verordnung, Basel-Stadt) and the Swiss animal protection law (Tierschutz-Gesetz).

Human Blood Specimens

Human PBMCs were isolated from healthy volunteers (males, 25-35 years old) or the *Coro1a*$^{-/-}$ individual (male, 20 years old) described earlier (Moshous et al., 2013) using a Histopaque 1077 (Sigma Aldrich, #10771) column following the manufacturers protocol.

Bacterial, viral and fungal strains:

Salmonella typhimurium; SL3261 (vaccine strain with aroA mutation), SL3261/pMW57 (vaccine strain expressing GFP-OVA from the in vivo inducible pagCp promoter) and SL1344 (wild-type virulent strain for challenge infection) *Staphylococcus aureus*; SH1000 strain for IV studies and SA113 WT for the foreign body infection model studies. *Candida albicans*; SC5314 strain. *Murine cytomegalovirus*; MCMV- Δ M157 strain.

Method Details

Reagents. Antibodies used were from the following sources: rabbit α-coronin 1 antibody (serum 1002) has been described before (Ferrari et al., 1999); mouse α-coronin 1 was from Abnova (Cat#H00011151-M01) or Abcam (Cat# ab56820). PDE4 antibody is from Abcam (ab14628). cAMP antibody (#sc-73761) and Phospho Thr^{196} CaMKIV antibody is from SCBT (SC28443). Anti CD80 (clone 16-10A1), α-CD86 (clone GL-1), hamster Isotype control (clone HTK888) and rat isotype control (clone RTK2071) were from Biolegend. Phospho Ser^{133} CREB antibody is from CST (#9196). CFSE and CTV is from Thermo Fisher scientific. All flow cytometry antibodies used were from Biolegend. H89, KN93 were purchased from Tocris Biosciences. Miglyol 812 is from IOI Oleo. DNase I (11284932001) is from Roche. 30 μm pre-separation filters (130-041-407) is from Miltenyi Biotech. Hyaluronidase type IV-S (H4271), Histopaque 1077 and kolliphor EL (C5315) are from Sigma. Collagenase type I (SCR103) and Actin antibody (MAB1501) is from Merck Millipore.

Heterotopic cardiac transplantation: Vascularized cardiac allografts were placed in the abdomen of recipient mice according to the method of Niimi et al. (Niimi, 2001). In brief, hearts from BALB/c donors were heterotopically transplanted into the abdominal cavity of WT and *Coro1a*$^{-/-}$ recipient (females, 8-10 weeks old) mice under anesthesia with the ascending aorta anastomosed to the native abdominal aorta and main pulmonary artery to the native inferior vena cava, and the pulmonary veins and vena cava of the graft were ligated. Heart graft survival was subsequently monitored daily by palpation, and the day of complete

cessation of heartbeat was considered as the day of rejection and was verified by autopsy. Loss of graft function within 48 h of transplant was considered a technical failure (<5% on average), and these animals were omitted from further analysis.

Skin transplantations and lymphoid organ analysis. Skin biopsies were grafted onto recipient mice following the procedure described before (Schmaler et al., 2014). In brief, under aseptic conditions, the donor mouse tail skin (1 cm^2) was transplanted onto the dorsum, about 2 cm below the ear line, of an anesthetized recipient mouse whose skin had been shaved and a small area (1 cm^2) removed to make space for the donor skin graft. The graft was glued using Histo-Acryl (Braun, # 1050052), bandaged and adequate analgesia (buprenorphine (50 μg/kg body weight) for 1 day and paracetamol (3 mg/kg body weight) for the next 5 days in drinking water) was provided. The bandage was removed 7 days later and the animals regularly monitored until the time of study termination depending on the status of the graft. H2-bm12 (I-A^{bm12}) tail skin grafts were used for major MHC mismatched studies. Skin grafts for minor histocompatibility-mismatched allograft studies were performed with tail skin from a C57BL/6 mice line ('minor' in short) generated in house by backcrossing four times the F1 (C57BL/6 x BALB/c) progeny to the C57BL/6 parental line (also see "mice" in Experimental Models, above). For adoptive transfer experiments, at the time indicated, the different populations of T cells as indicated were injected i.v. as described previously (Siegmund et al., 2011b). In case the animals showed graft removal immediately following bandage removal, poor health and/or aberrant behavior they were excluded from the analysis. Adoptive transfer of cells was

performed through tail vein using 200 µl volume of plain phenol red free RPMI using 26G needle fitted insulin syringes. Application of H89 (40 mg/kg body weight, B.D.) was started a day prior to adoptive transfer in 0.9% saline S.C. and maintained for 8 days, followed up by topical application on the allograft using a mixture of miglyol and kolliphor EL (1:1, 100 µL) to minimize development of rashes at the injection site. For analysis of immune cells, mice were euthanized with CO_2, and spleen and lymph nodes were harvested in ice cold PBS and smashed through a gridded mesh (steel/nylon (Sefar AG)). The debris were removed by a quick spin (300 *xg*, 10 sec). Spleen cells were treated with Ammonium-Chloride-Potassium (ACK) buffer (155mM NH_4Cl, 10mM $KHCO_2$, 1mM EDTA, pH 7.4) or BD FACS lysis buffer (#349202) to remove red blood cells. Cells were counted and stained in FACS buffer (PBS, 2% FCS, 5mM EDTA) with the appropriate antibodies. After incubation, cells were washed twice with the same buffer and resuspended in 200 µl of FACS buffer. The fluorescence was measured using a BD LSR Fortessa or BD FACS Canto cytometer and results analyzed using FlowJo software (Tree Star).

Immune cell infiltration inside allografts: The allografts were dissected out on day 8 post-surgical implantation on recipient mouse, minced into small pieces and incubated in digestion cocktail (Iscove's modified Dulbecco's medium containing DNase I (0.1 mg/ml), collagenase type I (3.3 mg/ml) and hyaluronidase type IV-S (1 mg/ml) (all from Sigma–Aldrich, St Louis, MO, USA) in a shaker bath at 37^{o}C for 90 min. The digested skin was subsequently crushed between Sefar mesh and filtered through a 30 µM pre-separation filter (Miltenyi Biotech), surface stained and assessed by flow cytometry.

T cell isolation: For biochemical experiments: T cells were purified from spleen by means of immuno-magnetic negative selection using total, CD4 or CD8 T cell isolation kits (Stemcell technologies) following the manufacturers protocol. The purity of the T cells used in any of the biochemical procedure mentioned was ~90% (as assessed by flow cytometry). *For adoptive transfer experiments:* T cells for adoptive transfer experiments were purified either by means of immuno-magnetic negative selection using total CD4 or CD8 T cell isolation kits (Stemcell technologies) or by means of surface staining and positive selection using flow cytometry-based cell sorting (BD FACS Aria). Depletion of $CD25^+$ T cells was performed by addition of biotinylated anti CD25 antibody (clone PC61, Biolegend) followed by addition of streptavidin beads and magnetic separation. The cells were re-suspended to appropriate numbers as mentioned in the Figure legend and injected intravenously through the tail vein in a volume of 200 µl/mouse. The purity of WT T cells and *Coro1a*$^{-/-}$ T cells used for adoptive transfer experiments were over 90% as assessed by flow cytometry.

Treg cell depletion protocol: Depletion of Treg cells with α-CD25 antibody (clone PC61) administration was performed as described in Siegmund et al (Siegmund et al., 2011a). In brief, *Coro1a*$^{-/-}$ mice and $RAG2^{-/-}$ controls that had been transplanted with minor histocompatibility antigen-mismatched skin transplant were subjected to α-CD25 antibody (clone PC61, 0.5 mg/mouse IP) administration to deplete regulatory T cells (on D-5, D-3). *Coro1a*$^{-/-}$ mice were subsequently bled on various days (D-5, D0, D21, D35 and D65) to assess the efficacy of PC61 mediated $CD25^+$ T cell depletion by α-CD25 antibody (clone

7D4) and re-administration of PC61 timed when an increase in Treg cell population was observed (on D36 and D66).

I*n vivo homeostatic proliferation inhibition:* The protocol was adapted from Sojka et al (Sojka et al., 2009). In brief, Ly5.1 WT $CD4^+$ T cells isolated by negative isolation from spleen and lymph nodes were surface labelled and FACS sorted for $CD4^+CD25^-CD62L^{hi}$ cells, CFSE labelled (5 µM, 5 minutes at room temperature), washed three times with plain RPMI medium and counted and resuspended to 1 million cells/ ml in plain RPMI. Likewise, Ly5.2 WT $CD4^+CD25^-$ $CD62L^{hi}$ cells (WT conventional T cells) were enriched and brought to 1 million cells/ml of plain RPMI media. *Coro1a*$^{-/-}$ $CD4^+$ T cells were negatively isolated and subsequently depleted of $CD25^+$ T cells using biotin labelled α-CD25 antibody followed by streptavidin dyna beads and MACS sorted. The cell purity was assessed by flow cytometry which revealed over 95% purity for all cell types. $RAG2^{-/-}$ mice were injected either only with $0.5x\ 10^6$ Ly5.1 $CD4^+CD25^-$ $CD62L^{hi}$ T cells or along with equal numbers of WT Ly5.2 $CD4^+CD25^-$ $CD62L^{hi}$ or cor $1^{-/-}$ Ly5.2 $CD4^+CD25^-$ cells through tail vein. Mice were sacrificed 7 days later (Fig 3 G,H) and the transferred Ly5.1 cells assessed by flow cytometry for CFSE dilution and their counts enumerated. For the data shown in Fig 3F, CD62L status was omitted and 1 million each of Ly5.1 and Ly5.2 cells were injected through the tail vein and analyzed on day 14.

Cell lysis and immunoblotting: Cells or tissues were lysed in Triton-X 100 buffer with 0.2% SDS containing protease and phosphatase inhibitors (Roche) at 4^oC as described (Jayachandran et al., 2014), followed by protein determination (BCA,

Pierce) and SDS-PAGE, transferred onto nitrocellulose and probed using the indicated antibodies followed by HRP-labeled secondary antibodies and developed using an enhanced chemi-luminescence imager (Fuji) as described before (Tulp et al., 1994) or using an IR dye tagged secondary antibody and imaged using a LI-COR imaging system.

Immunofluorescence analysis. Splenic T cells were fixed in PFA (4%) immediately for 20 min, followed by washing and saponin permeabilization (15 min 0.5%) when indicated. Following 30 min blocking with 2% BSA in PBS, cells were incubated with primary antibodies (1:1000, 1 h RT or overnight at 4°C) followed by Alexa Fluor 488 or -568 labeled secondary antibody incubation at room temperature for 1h. Jurkat cells were seeded on Poly-L-Lysine coated, 10 well Teflon coated slide (Thermo) for 1h at 37°C with 5% CO_2. The fixation was done with ice-cold 3% methanol, followed by washing in PBS-Dulbecco and blocked for 20 min with PBS-Dulbecco containing 5% FCS. The cells were then stained for coronin 1 using α-coronin 1 antibody (Abcam, 1:100 diluted in PBS-D/2%FCS) for 30 min at RT followed by Alexa fluor -568 conjugated secondary antibody (1:400, diluted in PBS-D/2% FCS) for 30 min at RT. DRAQ-5 (Biostatus) (1:1500, diluted in PBS-D/2% FCS) was used for 15 min at RT. Slides were analyzed using a LSM510 Meta confocal laser scanning microscope (Zeiss).

cAMP measurement: Total splenic T cells were isolated with the T cell isolation Kit (Stemcell technologies), according to the manufacturer's instruction. Cells were incubated with either DMSO or 100 µM rolipram (Tocris, #0905) in PBS/2% FCS/2 mM EDTA for 30 min at 37°C, 5% CO2. Cells were then

stimulated with 100 µM forskolin (Tocris, #1099) for 10 min at 37°C and lysed with Lysis Buffer/D2 solution from the HTRF cAMP femto 2 Kit (CisBio, #62AM5PEB) in 1.5 ml Eppendorf tubes. Lysates were then transferred to 384 plates (Greiner, #781075), Lysis Buffer/CC was added to each well and topped up with PBS/2% FCS/2 mM EDTA to a 20 µl final volume. Plates were incubated for 1 h at RT in the dark and measured on a Tecan Infinite F500 reader. Alternatively, cAMP levels determined using a cAMP ELISA kit following the manufacturers protocol (R&D systems, # SKGE002).

Protein kinase A activity measurement: PKA activity was measured using the Peptag® non-radioactive cAMP-dependent protein kinase as described before (Jayachandran et al., 2014). In brief, the non-radioactive PepTag PKA assay (Promega) was used to measure PKA activity from equal protein amounts of T cell lysates prepared in PKA extraction buffer (25 mM Tris-HCl (pH 7.4), 0.5 mM EDTA, 0.5 mM EGTA, 10 mM β-mercaptoethanol, 1 µg/ml leupeptin, 1 µg/ml aprotinin and 100 mM PMSF) to measure activity based on the phosphorylation of the fluorescent PKA substrate peptide, Leu-Arg-Arg-Ala-Ser-Leu-Gly (Kemptide), which, upon phosphorylation by PKA, acquires a negative charge and can be separated from the non-phosphorylated peptide by agarose gel electrophoresis. The in vitro phosphorylation of kemptide was performed for 30 minutes at 30 ^{o}C in a PCR machine, after which the samples were cooled to 4^{o} C, run on agarose gels and the phosphorylated band intensity quantitated and processed using Image J for assessment of PKA activity.

Genomic deletion of Coro1a in Jurkat T cells by CRISPR-Cas9 Genome Editing:

pSpCas9(BB)-2A-GFP (PX458) was a gift from Feng Zhang (Addgene plasmid # 48138). A 20-nucleotide sequence followed by a protospacer adjacent motif (PAM) from *Streptococcus pyogenes* targeting the third exon of human *Coro1a* was selected using publicly available tools: TTCATAGCACTGGTCGGCCTTGG as guide sequence was selected for the least number of potential off-target sites. The sequence was cloned into PX458 as previously described (Ran et al., 2013). Jurkat T cells ($2x10^6$) were electroporated with 20 µg of pX458-sgRNA plasmid at 250 volts for 5 ms using the Neon electroporation system (Invitrogen). GFP-expressing cells were sorted 48 h post-electroporation to enrich for transfected cells. Sorted cells were plated clonally at limiting dilution and screened by immunofluorescence staining against coronin 1. The absence of coronin 1 expression was further confirmed by immunoblotting.

Jurkat membrane fractionation and adenylate cyclase activity analysis: Jurkat cells were pelleted (200 *xg*/5'/4°C) and washed with Homogenization Buffer (HB) (10 mM Triethanolamine, 10 mM Acetic Acid, 1 mM EDTA, 0.25M Sucrose pH 7.4 supplemented with 50 µM NaF, 5 µM Na3Vo4 and Protease Inhibitors (Roche cOmplete #11873580001)) and resuspended in HB. Cells were homogenized using a 27G needle and homogenization was assessed under a microscope with trypan blue. Homogenate was then spun down for 10' at 1000 *xg* 4°C and post-nuclei supernatant transferred to a fresh ultracentrifuge 1.5 ml tube followed by another centrifugation for 30 min at 100'000 *xg*. The resulting membrane pellet was carefully resuspended with a 21G needle in 75 mM Tris pH 7.4, 12.5 mM $MgCl_2$, 1 mM EDTA supplemented with protease/phosphatase inhibitors (ThermoFisher HALT cocktail #78420). Protein concentrations were assessed by

BCA and equal µg of membranes were spun down for 15 min at 21'000 *xg*. The resulting pellet was resuspended in adenylate cyclase buffer (25 mM Tris pH 7.4, 5 mM $MgCl_2$, 1 mM EGTA, 1 mM DTT, 0.1 mg/ml BSA, 5 µM ATP) and stimulated with 100 µM FSK for 15 min at room temperature and the cAMP produced determined either using the cAMP HTRF kit or the cAMP ELISA as described under cAMP measurement.

Human PBMC and cAMP: For cAMP analysis, the isolated cells were subsequently analyzed by flow cytometry to characterize the various immune cell subtypes based on antibody staining for CD3, CD4, CD8, CD19 and CD25. Subsequently, these cells were serum starved for 2 h and subjected to 100 µM FSK stimulation and cAMP production assessed as shown in the section on *cAMP measurement*.

RNA sequencing analysis: WT or *Coro1a*$^{-/-}$ conventional T cells ($CD4^+CD25^-$) were enriched from spleen by negative isolation using the $CD4^+$ T cells isolation kit (Stemcell technologies) followed by depletion of $CD25^+$ T cells using biotinylated α-CD25 antibodies. Regulatory T cells ($CD4^+CD25^+$) were purified from spleen and lymph nodes of WT or *Coro1a*$^{-/-}$ mice by means of immuno-magnetic positive selection kit (Stemcell technologies) following the manufacturers protocol. The purity of conventional and regulatory T cells was over 90% (as assessed by flow cytometry). Total cellular RNA was isolated using TRIzol (Sigma), and the library generated with the Illumina TruSeq mRNA LT kit (poly-adenylated mRNA enriched) was sequenced in single read mode on an Illumina NextSeq 500 sequencing platform. Adaptor-trimmed reads were aligned to the *Mus musculus* genome (Ensembl GRCm38) using STAR (Dobin et al., 2013). Read

counts were summarized using htseq-count from the HTSeq package in union mode (Anders et al., 2015). Differential expression analysis was conducted using DESeq2 using a full model incorporating the effects of genotype, cell type, and the interaction of these variables with a cut-off of adjusted p-values < 0.05 (Love et al., 2014; Robinson et al., 2010; Yu and He, 2016; Yu et al., 2012). The PCA clustering of transcriptomes shown in Figure 3E was essentially identical when based on expression for all detected transcripts or those found to be differentially expressed.

Graft versus Host Disease (GvHD) analysis: Assessment of GvHD responses were performed as detailed in (Krenger et al., 2000a; Krenger et al., 2000b). In brief, total T cells were isolated from WT or *Coro1a*$^{-/-}$ C57BL/6 (I-A^{b}) mice by means of negative selection using Stem cell technologies kit (#19851) followed by CD25^{+} T cell depletion (see T cell isolation for adoptive transfer for more details). The isolated cells were transferred intravenously (20 x10^{6} cells) by means of tail vein injection into recipient BDF1 (I-A^{bd}) mice and kinetics of GvHD monitored. The parameters observed were weight loss, fur changes, immobility, skin rash, hair loss and loose stools. When the mice reached a weight loss of 20% the initial weight at day 0, the study was terminated and internal organs assessed for gross organomegaly, lymphadenopathy and thymic atrophy. The thymus was isolated, single cells prepared and stained for the CD3, CD4, CD8, TCRα and a viability marker to assess the double and single positive status along with cell viability and enumeration of total cell numbers. BDF1 mice receiving total splenocytes (35 x10^{6} cells), either from C57BL/6 (I-A^{b}) Ly5.1 mice or BDF1 (I-A^{bd}) mice served as positive (acute GvHD) and negative (no GvHD) controls.

In vitro T cell proliferation: WT or *Coro1a*$^{-/-}$ T cells isolated using the negative total T cell isolation kit (Stem cell technologies) were seeded on 96 well round bottom wells (2 x 10^5 cells/ well) at a final volume of 200 µl of RPMI supplemented with 10% FCS and penicillin-streptomycin (Sigma) and L-glutamine (Sigma) with plate bound CD3 (Biolegend, 10ug/ml in PBS for 2 h at 37^{o}C) and soluble α-CD28 (Biolegend, 2ug/ml) either in the presence of the PKA inhibitor H89 (1 µM, Tocris), the CaMKIV inhibitor KN93 (10 µM, Tocris), rolipram (5-1280 µM, Sigma) or vehicle only control. At 48 h time point, 1 µCi of tritiated thymidine was added to all wells and further incubated for 20 h followed by harvesting on a GF/C filter and measuring the DNA incorporated counts using a Packard instrument as a measure of T cell proliferation. Alternatively, T cells labelled with cell trace violet (CTV) were used and proliferation assessed by flow cytometry for CTV dilution.

Mixed Lymphocyte Reaction (MLR) in the presence of elevated cAMP: Total splenocytes were isolated from Balb/c mice (I-A^d), depleted of RBC using ACK lysis buffer (NH_4Cl (155 mM), KHCO2 (10 mM) and EDTA (1 mM)), counted and seeded in 12 well plate at 2 million cells/well in 2ml of APC medium (10% FCS containing DMEM with PSG (1x), Na-pyruvate (1x), NEAA (1x), L-Glutamine (1x) and β-ME (50 µM)). 24 hours later, these cells were collected, washed, counted and seeded at 0.1 million cells/well of a 96 well plate along with 0.1 million of CTV labelled C57BL/6 (I-A^b) WT T cells (purified using Total T cell isolation Kit, Stem Cell Technologies) in 200 µl volume of T cell medium (10% FCS containing RPMI with PSG (1x) + Na-pyruvate (1x) + NEAA (1x) + L-Glutamine (1x) + β-ME

(50 μM)) in the presence of blocking antibodies (α-CD80; 10 μg/ml and/or α-CD86; 10 μg/ml) or isotype controls (Iso Ctrl). Rolipram (10 μM) or DMSO controls were added in appropriate wells and after 84 h, the CD4 T cells were analyzed by flow cytometry for CTV dilution and analyzed using FlowJo (TreeStar).

Mixed Lymphocyte Reaction (MLR) with WT and Coro1a$^{-/-}$ APCs: Splenocytes were isolated from WT and *Coro1a*$^{-/-}$ mice C57BL/6 (I-A^{b}), depleted of RBC using ACK lysis buffer and used as APCs. APCs were seeded in 96-well round bottom plate starting from 0.2 million cells/well up to 25'000 cells/well along with 0.1 million of Balb/c mice (I-A^{d}) T cells (purified using Total T cell isolation Kit, Stem Cell Technologies) in a 200 μl volume of T cell medium for 3 days at the end of which 1 μCi of tritiated thymidine was added to all wells and further incubated for 20 h followed by harvesting on a GF/C filter and measuring the DNA incorporated counts using a Packard instrument as a measure of T cell proliferation.

T cell proliferation upon co-culture with Salmonella-*infected APCs*: Total splenocytes were isolated from Ly5.1 C57BL/6 mice (I-A^{b}), depleted of RBC using ACK lysis buffer (NH_4Cl (155mM), KHCO2 (10mM) and EDTA (1mM)), counted and seeded in overnight 10% FCS coated wells of a 12 well plate at 2 million cells/well in 2ml of APC medium (10% FCS containing DMEM with PSG (1x), Na-pyruvate (1x), NEAA (1x), L-Glutamine (1x) and β-ME (50 μM)) in the presence or absence of heat killed *Salmonella* (SL3261) or Ova-*Salmonella* (SL3261/pMW57) at a MOI of 1:50. 24 hours later, these cells were collected, washed, counted and seeded at 0.1 million cells/well of a 96 well plate along

with 0.1 million of CTV labelled Ly5.2 C57BL/6 (I-A^b) WT OTII T cells (purified using Total T cell isolation Kit, Stem Cell Technologies) in 200 l volume of T cell medium (10% FCS containing RPMI with PSG (1x) + Na-pyruvate (1x) + NEAA (1x) + L-Glutamine (1x) + β-ME (50 μM)). Rolipram (10 μM) or DMSO controls were added in appropriate wells and after 84 h, the ova-specific CD4 T cells responses were analyzed by flow cytometry for CTV dilution and analyzed using FlowJo (TreeStar).

In vivo APC activation: For allograft mediated activation: WT or *Coro1a*$^{-/-}$ mice were subjected to major MHC-mismatched BM12 allograft surgery and at day 8, the draining lymph nodes were analyzed. *For infection mediated activation:* WT and *Coro1a*$^{-/-}$ mice were injected s.c with 200 μl of heat killed *Salmonella* lysate (OD 2, in PBS, 85^o C for 1 h) in to the dorsal skin and after 4 days, the draining lymph nodes were analyzed for APC activation status as described above in the "*lymphoid organ analysis*".

MCMV Infection and analysis: Transgenic MCMV- Δ M157 (a kind gift from A. Oxenius (Bubic et al., 2004; Walton et al., 2008)) was propagated on mouse embryonic fibroblasts (MEF). MCMV titer was determined by a plaque assay. Methylcellulose was replaced by 3% Avicel RC-581. Mice were infected either intravenous (i.v.) into the tail vein. Mice were infected with 2 x 10^6 PFU of MCMV-ΔM157 i.v., Lungs, liver, spleen and salivary glands were harvested at the indicated time points (day 8, 26, 64 and 288) and viral titers were determined. MCMV-specific CD8 T cells in the blood were analyzed by flow cytometry using MCMV antigen (M45 and M38)-specific APC-conjugated tetramers at day 7 and

280 post infection. Naïve mice served as controls. Analysis of viral titers in the different organs was done essentially as described (Tchang et al., 2013).

Staphylococcus aureus and Candida albicans infections: WT or *Coro1a*$^{-/-}$ C57BL/6 mice were implanted subcutaneously on their dorsal surface with a Teflon catheter (BD Venflon, 15G, 1 cm length) with a defined inoculum of pathogen (*Candida albicans* (SC5314 strain); 1 x 10^4 and 1 x 10^7 CFU or *Staphylococcus aureus* (SA113 strain) 4.8x10^3 and 4.8 x 10^5 CFU) and followed up for kinetics of abscess formation using the foreign body infection model (Nowakowska et al., 2014). At the end of the study (day 15 for *S. aureus* and day 8 for *C. albicans*), mice were sacrificed and microorganisms adherent to the catheter, capsule around the catheter, soft tissue surrounding the catheter and blood (cardiac puncture) were enumerated by plating various dilutions. The mice were scored as follows; score 0: no abscess, score 1: slight edema, no abscess, score 3: abscess ≤ 3 mm (diameter 6 mm), score 6: abscess≥ 3 mm (diameter 6 mm).

Salmonella infection: For mice survival analysis with virulent *Salmonella*, WT or *Coro1a*$^{-/-}$ C57BL/6 mice were infected with *Salmonella* (*S. enterica* serovar Typhimurium, SL1344), 10^6 bacteria per oral and followed up for mice survival. The mice were monitored for signs of disease progression by recording the surface body temperature (infrared thermometer), fur signs, mobility and body weight. When the surface body temperature reached 30 degree Celsius, they were sacrificed and CFU load assessed from spleen and liver. For the vaccination-induced protection studies, the following *Salmonella* strains were used, SL3261

(10^9 bacilli, gastric inoculation, vaccine strain with aroA mutation (Hoiseth and Stocker, 1981)) and SL1344 (10^3 bacilli, i.v. inoculation via tail vein, wild-type virulent strain for challenge infection)(Bumann, 2001). For the OTII CD4 T cell response studies, OTII T cells (5 million) from either WT or *Coro1a*$^{-/-}$ mice were labeled with cell trace violet (CTV) and transferred into either C57BL/6 WT or *Coro1a*$^{-/-}$ mice respectively. Twenty-four hours later the mice were infected with either the normal *Salmonella* (SL3261, 10^9 bacilli, gastric inoculation) or GFP-OVA expressing *Salmonella* SL3261/pMW57 (10^9 bacilli, gastric inoculation, vaccine strain expressing GFP-OVA from the *in vivo* inducible *pagCp* promoter) (Bumann, 2001). The proliferation of transferred OT II T cells was monitored on day 7 from Payer's patches and mesenteric lymph nodes by flow cytometry. For the assessment of OVA-specific responses only those OTII cells that were labeled for CTV (CTV^{low} versus CTV^{high}) were considered. In parallel, on day 7 the CFUs were enumerated from spleen and liver.

Blood biochemistry profile analysis: The animals were sacrificed in a carbon dioxide chamber and immediately afterwards a cardiac puncture was performed and blood was aspirated and subjected to analysis in the biochemistry laboratory of the University Hospital Basel and the results compiled.

Analysis of microbiota in internal organs: For the analysis of various aerobic and anaerobic microbial floras in internal organs of the aged mice (> 30 weeks), the mice were sacrificed in a carbon dioxide chamber followed by dissection of the mice under sterile conditions for isolation of the duodenum and caecum. The organs were immediately minced into multiple small pieces in 500 µl of sterile

peptone water and a homogenous suspension was prepared. Various dilution of the suspension was plated in blood agar (aerobic and anaerobic conditions), McConkey agar (Enterobactericeae), Endoagar (Enterobactericeae), chromagar (Gram-positive bacteriae), Sabouraud agar (yeast and fungi). Appropriate incubation conditions were provided for both aerobic and anaerobic condition for 24-48 h after which, the colonies appearing were isolated and further identified by routine bacteriological characterization methods (MicroBioS GmbH, Switzerland).

Ageing and life expectancy studies: Age and sex matched WT and *Coro1a*$^{-/-}$ deficient mice (40 males and 40 females of either genotype) were housed in conventional animal cages (Techniplast) in groups of maximum 4 animals per cage and provided water and food *ad libitum*. They were scored regularly during their life span and monitored for general health status (grooming status, personal hygiene, discharge of purulent fluids from eyes, nose, anus, urethra, and skin rashes), altered stool stains in the holding cages, mobility, abdominal swelling, abnormal growth and fur changes. When mice became moribund due to ageing, they were sacrificed and internal organs analyzed for organomegaly, cysts, nodular deposits and hemorrhagic ascites. Histological assessment of any affected organ was performed as needed (Microbios GmBH).

Analysis of viral pathogens: For the analysis of various viral pathogens, aged mice (>30 weeks) were sacrificed in a carbon dioxide chamber and cardiac puncture was performed immediately to withdraw blood. The blood was allowed to clot and the serum was separated and the titer of antibodies against various common

mouse viral pathogens investigated as shown in table S2 (MicroBioS GmbH, Switzerland).

Histopathological analysis of various organs: For the analysis of various internal organs of the aged mice (>30 weeks), the mice were sacrificed in a carbon dioxide chamber followed by dissection of the mice under sterile conditions for isolation of the various internal solid organs including the liver, spleen, lungs, heart, pancreas, kidney and brain. The isolated organs were fixed in 4% formalin, sectioned and histochemistry analysis performed to assess any histological changes associated with malignant changes (MicroBioS GmbH, Switzerland).

Quantification and Statistical Analysis

Statistical analyses: Statistical analyses were performed with Prism (GraphPad Software) and Excel (Microsoft office). Gene ontology was performed using Panther (http://www.pantherdb.org/panther/ontologies.jsp. Comparisons between two groups were performed with the unpaired Student's *t*-test or the Mann-Whitney *U*-test (when the groups were independent and did not have a normal distribution) or using Log-rank (Mantel Cox analysis) for graft survival analysis. P values: * $P<0.05$, ** $P<0.01$, ***$P<0.001$ and ****$P<0.0001$. Error bars normally show standard deviation unless standard error margin is mentioned.

Data Availability

Data will be available from the Gene Expression Omnibus (GEO; GSE122567).

Author Contribution:

Skin transplant studies and analysis was performed by RJ, AG, BB, MSc and SRo. RJ, SRu, ML and SM performed the cAMP and PDE analysis. RJ and GF performed the RNAseq analysis. RJ, SD, AG, BB and GH contributed to the GvHD studies. MSt and SM generated the CRISPR-Cas9 *Coro1a*$^{-/-}$ Jurkat cell line. RJ, BC, AKW, VT, UK, NK, EM, DB performed the infection studies. RJ performed the PKA activity, MLR studies, pCREB blots, KN93, H89 proliferation and *in vivo* and *in vitro* rolipram studies. RJ and DM performed the human PBMC analysis. RJ and JP conceived, designed, analyzed and wrote the manuscript with input from all co-authors.

Acknowledgement

We thank Helene Rossez, Julie Ruer-Laventie, Lotte Kuhn, Janine Zankl, Stella Stefanova, Jiagui Li and Philippe Demougin for excellent support and assistance. We thank Bettina Oswald, Renato Zedi, Mattias Thimm, Frederic Schmitt, Dominique Grosshenny, David Ueberschlag and members of the Animal Unit, Biozentrum and DBM. We are indebted to Ed Palmer and the late Ton Rolink for fruitful discussions. RJ was supported by a Cloëtta foundation and Swiss Life fellowship. MS, BB and KS were supported by an HSFP fellowship, Marie Vögt Heim Fellowship, and Lise Meitner position of the FWF Austrian Science Fund respectively. This work was further supported by the Swiss National Science Foundation, the Gebert Ruef Foundation, the Swiss MS Society and the Canton of Basel. RNA sequencing was conducted at the Genomics Facility Basel (by Christian Beisel), ETH Zurich

Department of Biosystems Science and Engineering) and analyses were performed at sciCORE (http://scicore.unibas.ch/) scientific computing core facility at University of Basel, with support by the SIB Swiss Institute of Bioinformatics.

Declaration of Interests

Patents related to this work have been filed (WO2007110385A2 and WO2009112542A1) by the University of Basel. JP and RJ are co-founders of Leucogenics; NK is member of Advisory Boards of Basilea, Merck/MSD and Pfizer.

References:

Anders, S., Pyl, P.T., and Huber, W. (2015). HTSeq--a Python framework to work with high-throughput sequencing data. Bioinformatics *31*, 166-169.

Anderson, K.A., and Means, A.R. (2002). Defective signaling in a subpopulation of CD4(+) T cells in the absence of Ca(2+)/calmodulin-dependent protein kinase IV. Mol Cell Biol *22*, 23-29.

Anderson, K.A., Ribar, T.J., Illario, M., and Means, A.R. (1997). Defective survival and activation of thymocytes in transgenic mice expressing a catalytically inactive form of Ca2+/calmodulin-dependent protein kinase IV. Mol Endocrinol *11*, 725-737.

Arandjelovic, S., Wickramarachchi, D., Hemmers, S., Leming, S.S., Kono, D.H., and Mowen, K.A. (2010). Mast cell function is not altered by Coronin-1A deficiency. Journal of leukocyte biology *88*, 737-745.

Arumugham, V.B., and Baldari, C.T. (2017). cAMP: a multifaceted modulator of immune synapse assembly and T cell activation. J Leukoc Biol *101*, 1301-1316.

Avery, R.K. (2013). Update on infections in composite tissue allotransplantation. Curr Opin Organ Transplant *18*, 659-664.

Barnden, M.J., Allison, J., Heath, W.R., and Carbone, F.R. (1998). Defective TCR expression in transgenic mice constructed using cDNA-based alpha- and beta-chain genes under the control of heterologous regulatory elements. Immunology and cell biology *76*, 34-40.

Birkeland, S.A., Lokkegaard, H., and Storm, H.H. (2000). Cancer risk in patients on dialysis and after renal transplantation. Lancet *355*, 1886-1887.

Bodor, J., Bopp, T., Vaeth, M., Klein, M., Serfling, E., Hunig, T., Becker, C., Schild, H., and Schmitt, E. (2012). Cyclic AMP underpins suppression by regulatory T cells. Eur J Immunol *42*, 1375-1384.

Bopp, T., Becker, C., Klein, M., Klein-Hessling, S., Palmetshofer, A., Serfling, E., Heib, V., Becker, M., Kubach, J., Schmitt, S.*, et al.* (2007). Cyclic adenosine monophosphate is a key component of regulatory T cell-mediated suppression. J Exp Med *204*, 1303-1310.

Bourne, H.R., Lichtenstein, L.M., Melmon, K.L., Henney, C.S., Weinstein, Y., and Shearer, G.M. (1974). Modulation of inflammation and immunity by cyclic AMP. Science *184*, 19-28.

Bubic, I., Wagner, M., Krmpotic, A., Saulig, T., Kim, S., Yokoyama, W.M., Jonjic, S., and Koszinowski, U.H. (2004). Gain of virulence caused by loss of a gene in murine cytomegalovirus. J Virol *78*, 7536-7544.

Bumann, D. (2001). Regulated antigen expression in live recombinant Salmonella enterica serovar Typhimurium strongly affects colonization capabilities and specific CD4(+)-T-cell responses. Infect Immun *69*, 7493-7500.

Combaluzier, B., Mueller, P., Massner, J., Finke, D., and Pieters, J. (2009). Coronin 1 is essential for IgM-mediated Ca2+ mobilization in B cells but dispensable for the generation of immune responses in vivo. J Immunol *182*, 1954-1961.

Combaluzier, B., and Pieters, J. (2009). Chemotaxis and phagocytosis in neutrophils is independent of coronin 1. J Immunol *182*, 2745-2752.

Dobin, A., Davis, C.A., Schlesinger, F., Drenkow, J., Zaleski, C., Jha, S., Batut, P., Chaisson, M., and Gingeras, T.R. (2013). STAR: ultrafast universal RNA-seq aligner. Bioinformatics *29*, 15-21.

Doherty, P.C., and Zinkernagel, R.M. (1975). A biological role for the major histocompatibility antigens. Lancet *1*, 1406-1409.

Dupre, D.J., Robitaille, M., Rebois, R.V., and Hebert, T.E. (2009). The role of Gbetagamma subunits in the organization, assembly, and function of GPCR signaling complexes. Annu Rev Pharmacol Toxicol *49*, 31-56.

Erdogan, S., and Houslay, M.D. (1997). Challenge of human Jurkat T-cells with the adenylate cyclase activator forskolin elicits major changes in cAMP phosphodiesterase (PDE) expression by up-regulating PDE3 and inducing PDE4D1 and PDE4D2 splice variants as well as down-regulating a novel PDE4A splice variant. Biochem J *321 (Pt 1)*, 165-175.

Ferrari, G., Langen, H., Naito, M., and Pieters, J. (1999). A coat protein on phagosomes involved in the intracellular survival of mycobacteria. Cell *97*, 435-447.

Foger, N., Rangell, L., Danilenko, D.M., and Chan, A.C. (2006). Requirement for coronin 1 in T lymphocyte trafficking and cellular homeostasis. Science *313*, 839-842.

Ford, M.L. (2016). T Cell Cosignaling Molecules in Transplantation. Immunity *44*, 1020-1033.

Fulton, L.M., Taylor, N.A., Coghill, J.M., West, M.L., Foger, N., Bear, J.E., Baldwin, A.S., Panoskaltsis-Mortari, A., and Serody, J.S. (2014). Altered T-cell entry and egress in the absence of Coronin 1A attenuates murine acute graft versus host disease. Eur J Immunol *44*, 1662-1671.

Giembycz, M.A., Corrigan, C.J., Seybold, J., Newton, R., and Barnes, P.J. (1996). Identification of cyclic AMP phosphodiesterases 3, 4 and 7 in human CD4+ and CD8+ T-lymphocytes: role in regulating proliferation and the biosynthesis of interleukin-2. Br J Pharmacol *118*, 1945-1958.

Goldrath, A.W., and Bevan, M.J. (1999). Selecting and maintaining a diverse T-cell repertoire. Nature *402*, 255-262.

Goulmy, E., Schipper, R., Pool, J., Blokland, E., Falkenburg, J.H., Vossen, J., Gratwohl, A., Vogelsang, G.B., van Houwelingen, H.C., and van Rood, J.J. (1996). Mismatches of minor histocompatibility antigens between HLA-identical donors and recipients and the development of graft-versus-host disease after bone marrow transplantation. N Engl J Med *334*, 281-285.

Haraldsson, M.K., Louis-Dit-Sully, C.A., Lawson, B.R., Sternik, G., Santiago-Raber, M.L., Gascoigne, N.R., Theofilopoulos, A.N., and Kono, D.H. (2008). The lupus-related Lmb3 locus contains a disease-suppressing Coronin-1A gene mutation. Immunity *28*, 40-51.

Hoiseth, S.K., and Stocker, B.A. (1981). Aromatic-dependent Salmonella typhimurium are non-virulent and effective as live vaccines. Nature *291*, 238-239.

Huseby, E.S., White, J., Crawford, F., Vass, T., Becker, D., Pinilla, C., Marrack, P., and Kappler, J.W. (2005). How the T cell repertoire becomes peptide and MHC specific. Cell *122*, 247-260.

Jayachandran, R., Liu, X., Bosedasgupta, S., Muller, P., Zhang, C.L., Moshous, D., Studer, V., Schneider, J., Genoud, C., Fossoud, C.*, et al.* (2014). Coronin 1 Regulates Cognition and Behavior through Modulation of cAMP/Protein Kinase A Signaling. PLoS Biol *12*, e1001820.

Jayachandran, R., Sundaramurthy, V., Combaluzier, B., Mueller, P., Korf, H., Huygen, K., Miyazaki, T., Albrecht, I., Massner, J., and Pieters, J. (2007). Survival of mycobacteria in macrophages is mediated by coronin 1-dependent activation of calcineurin. Cell *130*, 37-50.

Josefowicz, S.Z., Lu, L.F., and Rudensky, A.Y. (2012). Regulatory T cells: mechanisms of differentiation and function. Annu Rev Immunol *30*, 531-564.

Klenerman, P., and Oxenius, A. (2016). T cell responses to cytomegalovirus. Nat Rev Immunol *16*, 367-377.

Krenger, W., Rossi, S., and Hollander, G.A. (2000a). Apoptosis of thymocytes during acute graft-versus-host disease is independent of glucocorticoids. Transplantation *69*, 2190-2193.

Krenger, W., Rossi, S., Piali, L., and Hollander, G.A. (2000b). Thymic atrophy in murine acute graft-versus-host disease is effected by impaired cell cycle progression of host pro-T and pre-T cells. Blood *96*, 347-354.

Krumins, A.M., and Gilman, A.G. (2006). Targeted knockdown of G protein subunits selectively prevents receptor-mediated modulation of effectors and reveals complex changes in non-targeted signaling proteins. J Biol Chem *281*, 10250-10262.

Kupz, A., Bedoui, S., and Strugnell, R.A. (2014). Cellular requirements for systemic control of Salmonella enterica serovar Typhimurium infections in mice. Infect Immun *82*, 4997-5004.

Lang, M.J., Mori, M., Ruer-Laventie, J., and Pieters, J. (2017). A Coronin 1-Dependent Decision Switch in Juvenile Mice Determines the Population of the Peripheral Naive T Cell Compartment. J Immunol *199*, 2421-2431.

Love, M.I., Huber, W., and Anders, S. (2014). Moderated estimation of fold change and dispersion for RNA-seq data with DESeq2. Genome Biol *15*, 550.

Mace, E.M., and Orange, J.S. (2014). Lytic immune synapse function requires filamentous actin deconstruction by Coronin 1A. Proc Natl Acad Sci U S A *111*, 6708-6713.

McKenzie, I.F., Morgan, G.M., Sandrin, M.S., Michaelides, M.M., Melvold, R.W., and Kohn, H.I. (1979). B6.C-H-2bm12. A new H-2 mutation in the I region in the mouse. J Exp Med *150*, 1323-1338.

Mosenden, R., and Tasken, K. (2011). Cyclic AMP-mediated immune regulation--overview of mechanisms of action in T cells. Cell Signal *23*, 1009-1016.

Moshous, D., Martin, E., Carpentier, W., Lim, A., Callebaut, I., Canioni, D., Hauck, F., Majewski, J., Schwartzentruber, J., Nitschke, P.*, et al.* (2013). Whole-exome sequencing identifies Coronin-1A deficiency in 3 siblings with immunodeficiency and EBV-associated B-cell lymphoproliferation. J Allergy Clin Immunol *131*, 1594-1603.

Mueller, P., Liu, X., and Pieters, J. (2011). Migration and homeostasis of naive T cells depends on coronin 1-mediated prosurvival signals and not on coronin 1-dependent filamentous actin modulation. J Immunol *186*, 4039-4050.

Mueller, P., Massner, J., Jayachandran, R., Combaluzier, B., Albrecht, I., Gatfield, J., Blum, C., Ceredig, R., Rodewald, H.R., Rolink, A.G.*, et al.* (2008). Regulation of T cell survival through coronin-1-mediated generation of inositol-1,4,5-trisphosphate and calcium mobilization after T cell receptor triggering. Nat Immunol *9*, 424-431.

Niimi, M. (2001). The technique for heterotopic cardiac transplantation in mice: experience of 3000 operations by one surgeon. J Heart Lung Transplant *20*, 1123-1128.

Nowakowska, J., Landmann, R., and Khanna, N. (2014). Foreign Body Infection Models to Study Host-Pathogen Response and Antimicrobial Tolerance of Bacterial Biofilm. Antibiotics (Basel) *3*, 378-397.

Omori, K., and Kotera, J. (2007). Overview of PDEs and their regulation. Circ Res *100*, 309-327.

Pick, R., Begandt, D., Stocker, T.J., Salvermoser, M., Thome, S., Bottcher, R.T., Montanez, E., Harrison, U., Forne, I., Khandoga, A.G., *et al.* (2017). Coronin 1A, a novel player in integrin biology, controls neutrophil trafficking in innate immunity. Blood *130*, 847-858.

Punwani, D., Pelz, B., Yu, J., Arva, N.C., Schafernak, K., Kondratowicz, K., Makhija, M., and Puck, J.M. (2015). Coronin-1A: Immune Deficiency in Humans and Mice. J Clin Immunol.

Ran, F.A., Hsu, P.D., Wright, J., Agarwala, V., Scott, D.A., and Zhang, F. (2013). Genome engineering using the CRISPR-Cas9 system. Nat Protoc *8*, 2281-2308.

Ravindran, R., and McSorley, S.J. (2005). Tracking the dynamics of T-cell activation in response to Salmonella infection. Immunology *114*, 450-458.

Richters, C.D., Hoekstra, M.J., du Pont, J.S., Kreis, R.W., and Kamperdijk, E.W. (2005). Immunology of skin transplantation. Clin Dermatol *23*, 338-342.

Robinson, M.D., McCarthy, D.J., and Smyth, G.K. (2010). edgeR: a Bioconductor package for differential expression analysis of digital gene expression data. Bioinformatics *26*, 139-140.

Sakaguchi, S., Yamaguchi, T., Nomura, T., and Ono, M. (2008). Regulatory T cells and immune tolerance. Cell *133*, 775-787.

Schmaler, M., Broggi, M.A., and Rossi, S.W. (2014). Transplantation of tail skin to study allogeneic CD4 T cell responses in mice. J Vis Exp, e51724.

Schmidt, E.M., Wang, C.J., Ryan, G.A., Clough, L.E., Qureshi, O.S., Goodall, M., Abbas, A.K., Sharpe, A.H., Sansom, D.M., and Walker, L.S. (2009). Ctla-4 controls regulatory T cell peripheral homeostasis and is required for suppression of pancreatic islet autoimmunity. J Immunol *182*, 274-282.

Shinkai, Y., Rathbun, G., Lam, K.P., Oltz, E.M., Stewart, V., Mendelsohn, M., Charron, J., Datta, M., Young, F., Stall, A.M., *et al.* (1992). RAG-2-deficient mice lack mature lymphocytes owing to inability to initiate V(D)J rearrangement. Cell *68*, 855-867.

Shiow, L.R., Paris, K., Akana, M.C., Cyster, J.G., Sorensen, R.U., and Puck, J.M. (2009). Severe combined immunodeficiency (SCID) and attention deficit hyperactivity disorder (ADHD) associated with a Coronin-1A mutation and a chromosome 16p11.2 deletion. Clin Immunol *131*, 24-30.

Shiow, L.R., Roadcap, D.W., Paris, K., Watson, S.R., Grigorova, I.L., Lebet, T., An, J., Xu, Y., Jenne, C.N., Foger, N., *et al.* (2008). The actin regulator coronin 1A is mutant in a thymic egress-deficient mouse strain and in a patient with severe combined immunodeficiency. Nat Immunol *9*, 1307-1315.

Siegmund, K., Lee, W.Y., Tchang, V.S., Stiess, M., Terracciano, L., Kubes, P., and Pieters, J. (2013). Coronin 1 is dispensable for leukocyte recruitment and liver injury in concanavalin A-induced hepatitis. Immunol Lett *153*, 62-70.

Siegmund, K., Zeis, T., Kunz, G., Rolink, T., Schaeren-Wiemers, N., and Pieters, J. (2011a). Coronin 1-mediated naive T cell survival is essential for the development of autoimmune encephalomyelitis. J Immunol *186*, 3452-3461.

Siegmund, K., Zeis, T., Kunz, G., Rolink, T., Schaeren-Wiemers, N., and Pieters, J. (2011b). Coronin 1-mediated naive T cell survival is essential for the development of autoimmune encephalomyelitis. Journal of immunology *186*, 3452-3461.

Soderling, T.R. (1999). The Ca-calmodulin-dependent protein kinase cascade. Trends Biochem Sci *24*, 232-236.

Sojka, D.K., Hughson, A., and Fowell, D.J. (2009). CTLA-4 is required by CD4+CD25+ Treg to control CD4+ T-cell lymphopenia-induced proliferation. Eur J Immunol *39*, 1544-1551.

Stray-Pedersen, A., Jouanguy, E., Crequer, A., Bertuch, A.A., Brown, B.S., Jhangiani, S.N., Muzny, D.M., Gambin, T., Sorte, H., Sasa, G.*, et al.* (2014). Compound heterozygous CORO1A mutations in siblings with a mucocutaneous-immunodeficiency syndrome of epidermodysplasia verruciformis-HPV, molluscum contagiosum and granulomatous tuberculoid leprosy. J Clin Immunol *34*, 871-890.

Suo, D., Park, J., Harrington, A.W., Zweifel, L.S., Mihalas, S., and Deppmann, C.D. (2014). Coronin-1 is a neurotrophin endosomal effector that is required for developmental competition for survival. Nat Neurosci *17*, 36-45.

Surh, C.D., and Sprent, J. (2008). Homeostasis of naive and memory T cells. Immunity *29*, 848-862.

Tang, Q., and Bluestone, J.A. (2013). Regulatory T-cell therapy in transplantation: moving to the clinic. Cold Spring Harb Perspect Med *3*.

Tao, R., de Zoeten, E.F., Ozkaynak, E., Chen, C., Wang, L., Porrett, P.M., Li, B., Turka, L.A., Olson, E.N., Greene, M.I.*, et al.* (2007). Deacetylase inhibition promotes the generation and function of regulatory T cells. Nat Med *13*, 1299-1307.

Taylor, S.S., Kim, C., Vigil, D., Haste, N.M., Yang, J., Wu, J., and Anand, G.S. (2005). Dynamics of signaling by PKA. Biochim Biophys Acta *1754*, 25-37.

Tchang, V.S., Mekker, A., Siegmund, K., Karrer, U., and Pieters, J. (2013). Diverging role for coronin 1 in antiviral CD4+ and CD8+ T cell responses. Mol Immunol *56*, 683-692.

Tchang, V.S., Stiess, M., Siegmund, K., Karrer, U., and Pieters, J. (2017). Role for coronin 1 in mouse NK cell function. Immunobiology *222*, 291-300.

Tulp, A., Verwoerd, D., Dobberstein, B., Ploegh, H.L., and Pieters, J. (1994). Isolation and characterization of the intracellular MHC class II compartment. Nature *369*, 120-126.

Vang, T., Torgersen, K.M., Sundvold, V., Saxena, M., Levy, F.O., Skalhegg, B.S., Hansson, V., Mustelin, T., and Tasken, K. (2001). Activation of the COOH-terminal Src kinase (Csk) by cAMP-dependent protein kinase inhibits signaling through the T cell receptor. J Exp Med *193*, 497-507.

Verma, S., Weiskopf, D., Gupta, A., McDonald, B., Peters, B., Sette, A., and Benedict, C.A. (2015). Cytomegalovirus-Specific CD4 T Cells Are Cytolytic and Mediate Vaccine Protection. J Virol *90*, 650-658.

Vinet, A.F., Fiedler, T., Studer, V., Froquet, R., Dardel, A., Cosson, P., and Pieters, J. (2014). Initiation of multicellular differentiation in Dictyostelium discoideum is regulated by coronin A. Mol Biol Cell *25*, 688-701.

Walton, S.M., Wyrsch, P., Munks, M.W., Zimmermann, A., Hengel, H., Hill, A.B., and Oxenius, A. (2008). The dynamics of mouse cytomegalovirus-specific CD4 T cell responses during acute and latent infection. J Immunol *181*, 1128-1134.

Wayman, G.A., Tokumitsu, H., and Soderling, T.R. (1997). Inhibitory cross-talk by cAMP kinase on the calmodulin-dependent protein kinase cascade. J Biol Chem *272*, 16073-16076.

Wehbi, V.L., and Tasken, K. (2016). Molecular Mechanisms for cAMP-Mediated Immunoregulation in T cells - Role of Anchored Protein Kinase A Signaling Units. Front Immunol *7*, 222.

Westritschnig, K., BoseDasgupta, S., Tchang, V., Siegmund, K., and Pieters, J. (2013). Antigen processing and presentation by dendritic cells is independent of coronin 1. Molecular immunology *53*, 379-386.

Yee, C.S., Massaad, M.J., Bainter, W., Ohsumi, T.K., Foger, N., Chan, A.C., Akarsu, N.A., Aytekin, C., Ayvaz, D.C., Tezcan, I.*, et al.* (2016). Recurrent viral infections associated with a homozygous CORO1A mutation that disrupts oligomerization and cytoskeletal association. J Allergy Clin Immunol *137*, 879-888 e872.

Yu, G., and He, Q.Y. (2016). ReactomePA: an R/Bioconductor package for reactome pathway analysis and visualization. Mol Biosyst *12*, 477-479.

Yu, G., Wang, L.G., Han, Y., and He, Q.Y. (2012). clusterProfiler: an R package for comparing biological themes among gene clusters. OMICS *16*, 284-287.

Zheng, X.X., Sayegh, M.H., Zheng, X.G., Li, Y., Linsley, P.S., Peach, R., Borriello, F., Strom, T.B., Sharpe, A.H., and Turka, L.A. (1997). The role of donor and recipient B7-1 (CD80) in allograft rejection. J Immunol *159*, 1169-1173.

Ziegler, C., Goldmann, O., Hobeika, E., Geffers, R., Peters, G., and Medina, E. (2011). The dynamics of T cells during persistent Staphylococcus aureus infection: from antigen-reactivity to in vivo anergy. EMBO Mol Med *3*, 652-666.

Zinkernagel, R.M., and Doherty, P.C. (1979). MHC-restricted cytotoxic T cells: studies on the biological role of polymorphic major transplantation antigens determining T-cell restriction-specificity, function, and responsiveness. Adv Immunol *27*, 51-177.

Figure 1

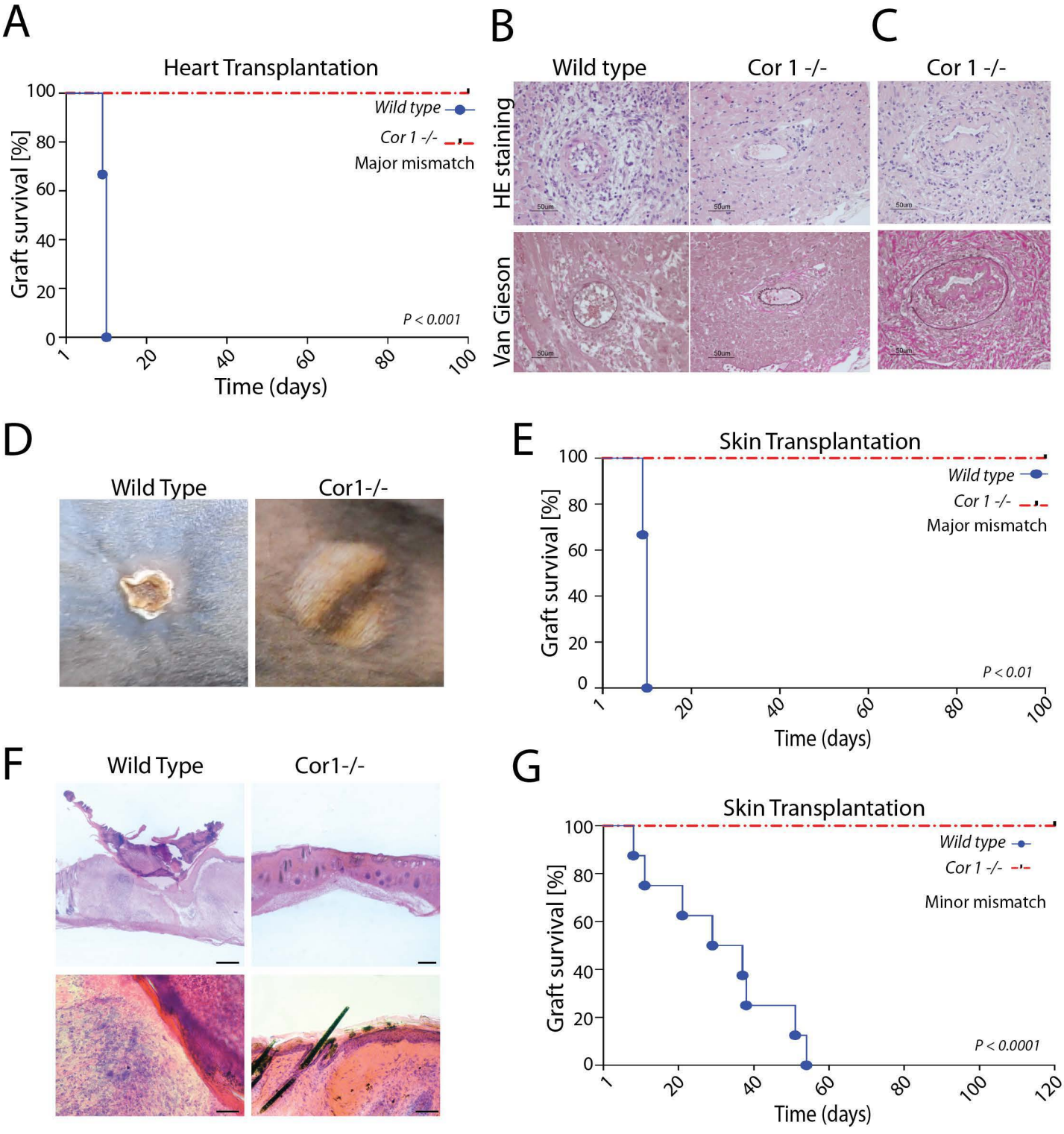
A
Heart Transplantation
Graft survival [%]
Time (days)
Wild type
Cor 1 -/-
Major mismatch
P < 0.001
B
Wild type
Cor 1 -/-
HE staining
Van Gieson
C
Cor 1 -/-
D
Wild Type
Cor1-/-
E
Skin Transplantation
Graft survival [%]
Time (days)
Wild type
Cor 1 -/-
Major mismatch
P < 0.01
F
Wild Type
Cor1-/-
G
Skin Transplantation
Graft survival [%]
Time (days)
Wild type
Cor 1 -/-
Minor mismatch
P < 0.0001

Figure 2

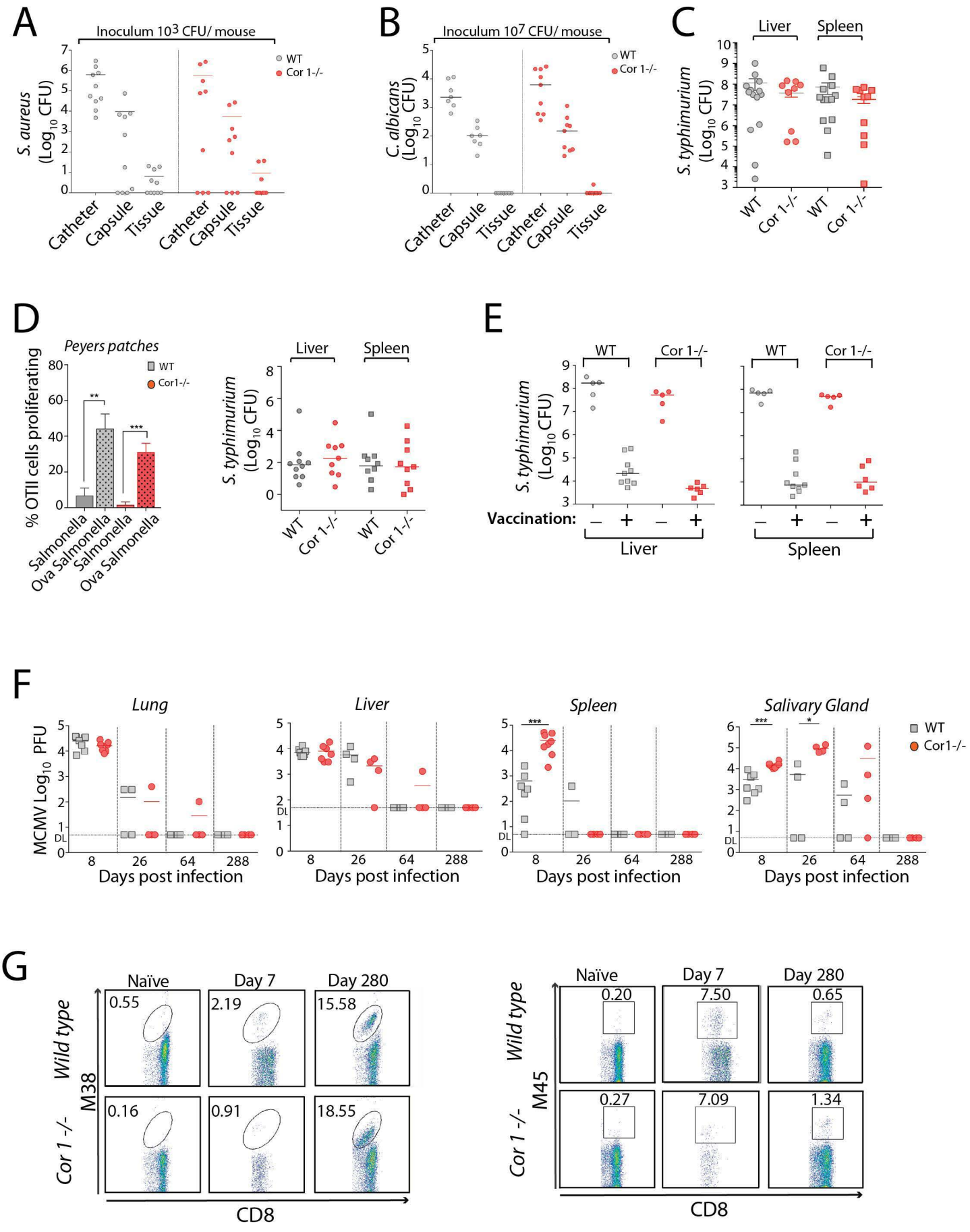
A
Inoculum 10^3 CFU/ mouse
S. aureus (Log10 CFU)
WT
Cor 1-/-
Catheter
Capsule
Tissue
B
Inoculum 10^7 CFU/ mouse
C. albicans (Log10 CFU)
C
Liver
Spleen
S. typhimurium (Log10 CFU)
D
Peyers patches
% OTII cells proliferating
Salmonella
Ova Salmonella
E
Vaccination:
F
Lung
Liver
Spleen
Salivary Gland
MCMV Log10 PFU
DL
Days post infection
G
Naïve
Day 7
Day 280
Wild type
Cor 1 -/-
M38
M45
CD8
0.55
2.19
15.58
0.16
0.91
18.55
0.20
7.50
0.65
0.27
7.09
1.34

Figure 3

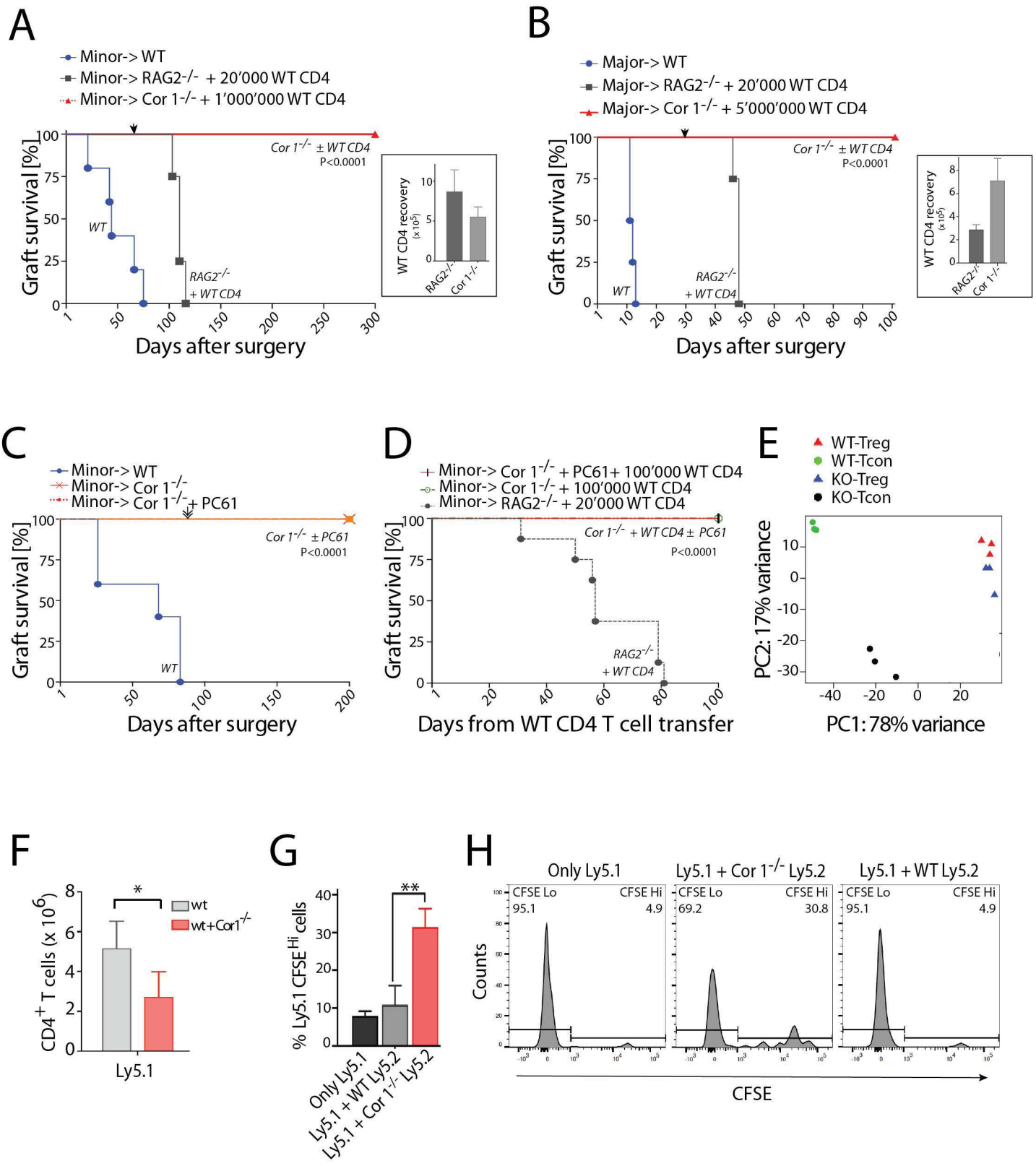
A
Minor-> WT
Minor-> RAG2-/- + 20'000 WT CD4
Minor-> Cor 1-/- + 1'000'000 WT CD4
Graft survival [%]
Cor 1-/- ± WT CD4
P<0.0001
WT
RAG2-/- + WT CD4
Days after surgery
WT CD4 recovery (x 10^5)
RAG2-/-
Cor 1-/-
B
Major-> WT
Major-> RAG2-/- + 20'000 WT CD4
Major-> Cor 1-/- + 5'000'000 WT CD4
Graft survival [%]
Cor 1-/- ± WT CD4
P<0.0001
WT
RAG2-/- + WT CD4
Days after surgery
WT CD4 recovery (x 10^5)
RAG2-/-
Cor 1-/-
C
Minor-> WT
Minor-> Cor 1-/-
Minor-> Cor 1-/- + PC61
Graft survival [%]
Cor 1-/- ± PC61
P<0.0001
WT
Days after surgery
D
Minor-> Cor 1-/- + PC61+ 100'000 WT CD4
Minor-> Cor 1-/- + 100'000 WT CD4
Minor-> RAG2-/- + 20'000 WT CD4
Graft survival [%]
Cor 1-/- + WT CD4 ± PC61
P<0.0001
RAG2-/- + WT CD4
Days from WT CD4 T cell transfer
E
WT-Treg
WT-Tcon
KO-Treg
KO-Tcon
PC2: 17% variance
PC1: 78% variance
F
CD4+ T cells (x 10^6)
wt
wt+Cor1-/-
Ly5.1
G
% Ly5.1 CFSE^Hi cells
Only Ly5.1
Ly5.1 + WT Ly5.2
Ly5.1 + Cor 1-/- Ly5.2
H
Only Ly5.1
Ly5.1 + Cor 1-/- Ly5.2
Ly5.1 + WT Ly5.2
CFSE Lo
CFSE Hi
95.1
4.9
69.2
30.8
95.1
4.9
Counts
CFSE

Figure 4

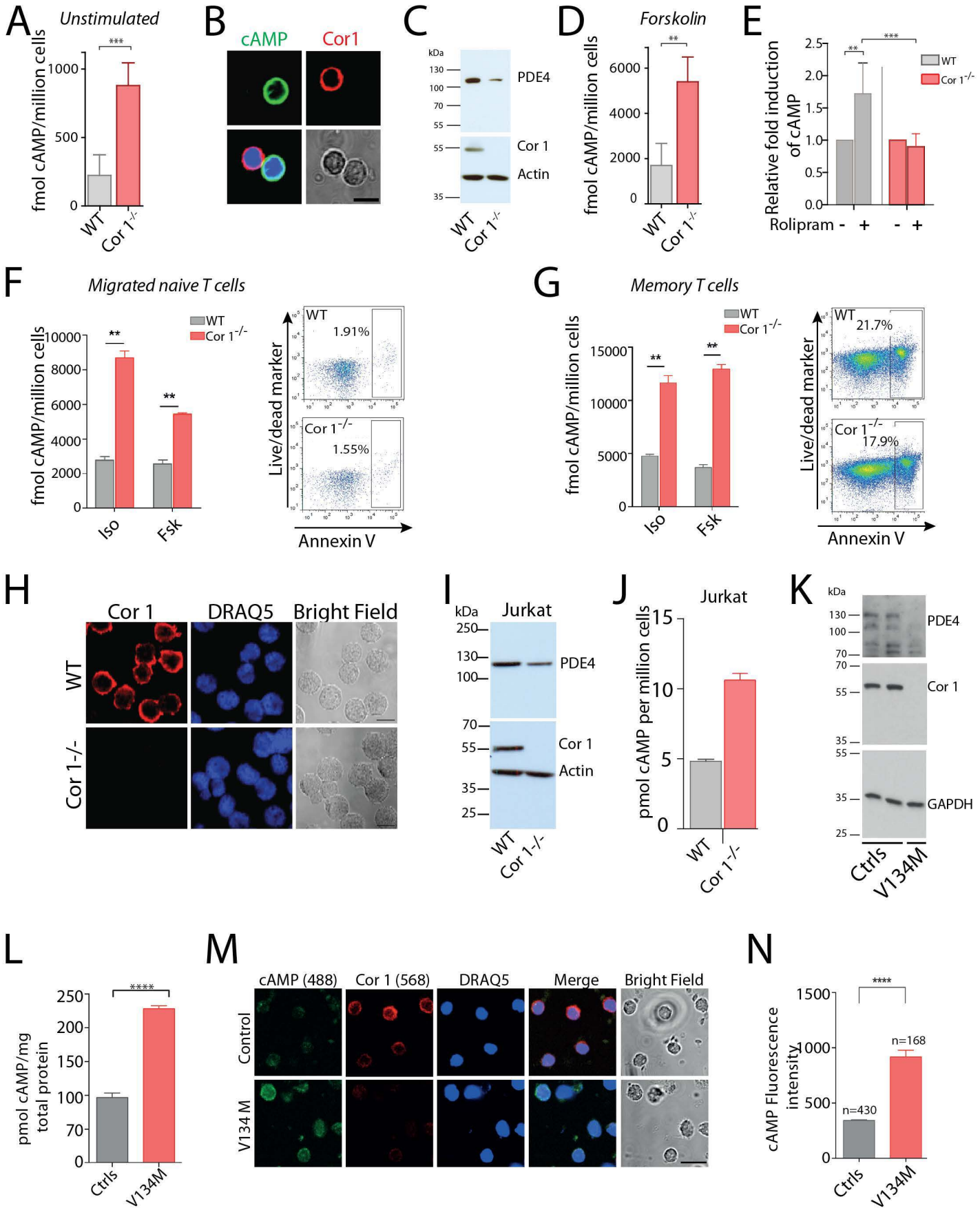
A
Unstimulated
fmol cAMP/million cells
WT
Cor 1-/-
B
cAMP
Cor1
C
kDa
PDE4
Cor 1
Actin
D
Forskolin
fmol cAMP/million cells
E
Relative fold induction of cAMP
Rolipram
F
Migrated naive T cells
fmol cAMP/million cells
Iso
Fsk
Live/dead marker
Annexin V
1.91%
1.55%
G
Memory T cells
21.7%
17.9%
H
Cor 1
DRAQ5
Bright Field
I
Jurkat
J
pmol cAMP per million cells
K
GAPDH
Ctrls
V134M
L
pmol cAMP/mg total protein
M
cAMP (488)
Cor 1 (568)
Merge
Control
V134 M
N
cAMP Fluorescence intensity
n=430
n=168

Figure 5

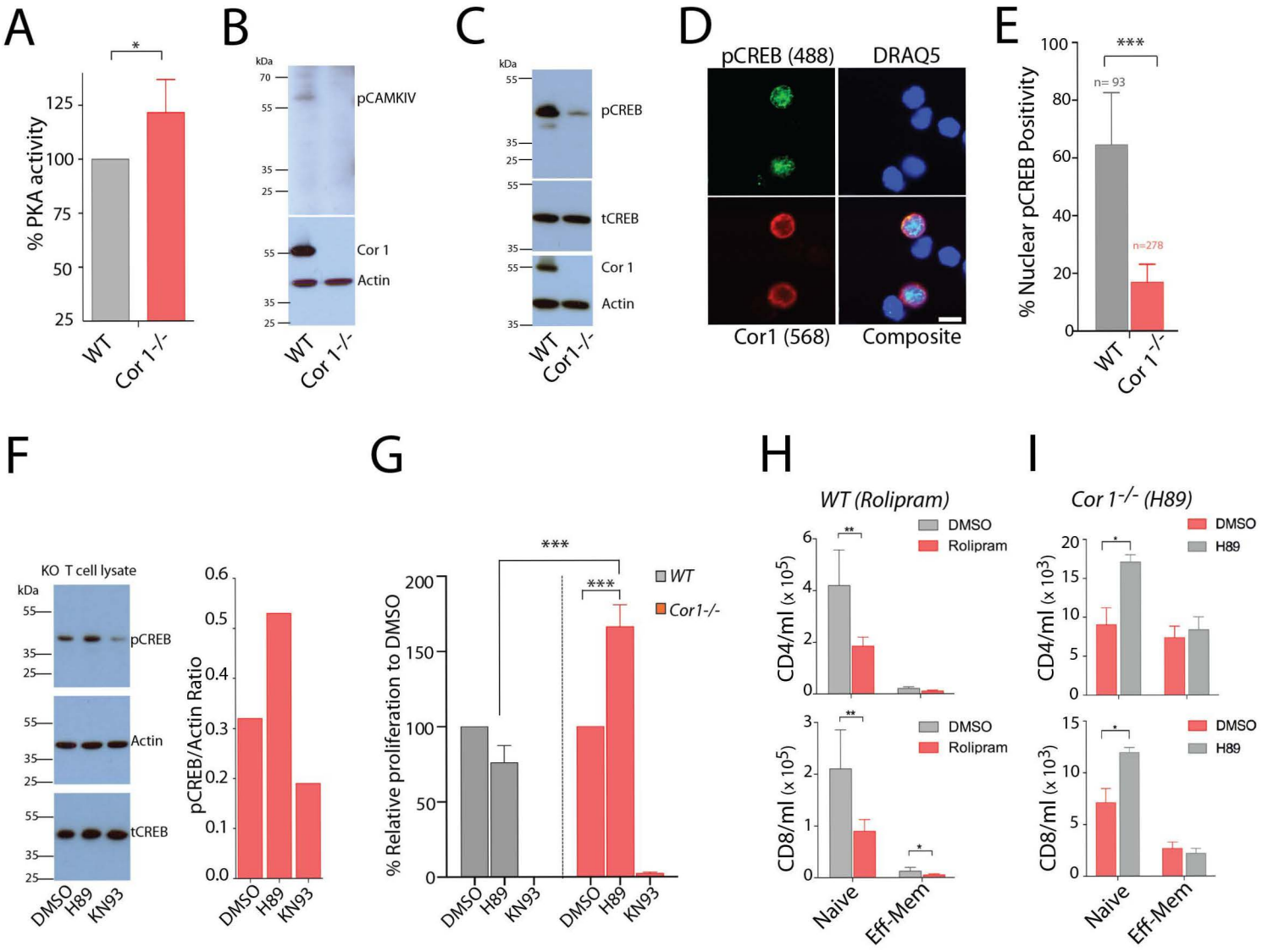
A
B
C
D
E
F
G
H
I
% PKA activity
WT
Cor 1-/-
pCAMKIV
Cor 1
Actin
kDa
pCREB
tCREB
pCREB (488)
DRAQ5
Cor1 (568)
Composite
% Nuclear pCREB Positivity
n= 93
n=278
KO T cell lysate
pCREB/Actin Ratio
DMSO
H89
KN93
% Relative proliferation to DMSO
WT
Cor1-/-
WT (Rolipram)
Cor 1-/- (H89)
CD4/ml (x 10^5)
CD8/ml (x 10^5)
CD4/ml (x 10^3)
CD8/ml (x 10^3)
Rolipram
Naive
Eff-Mem

Figure 6

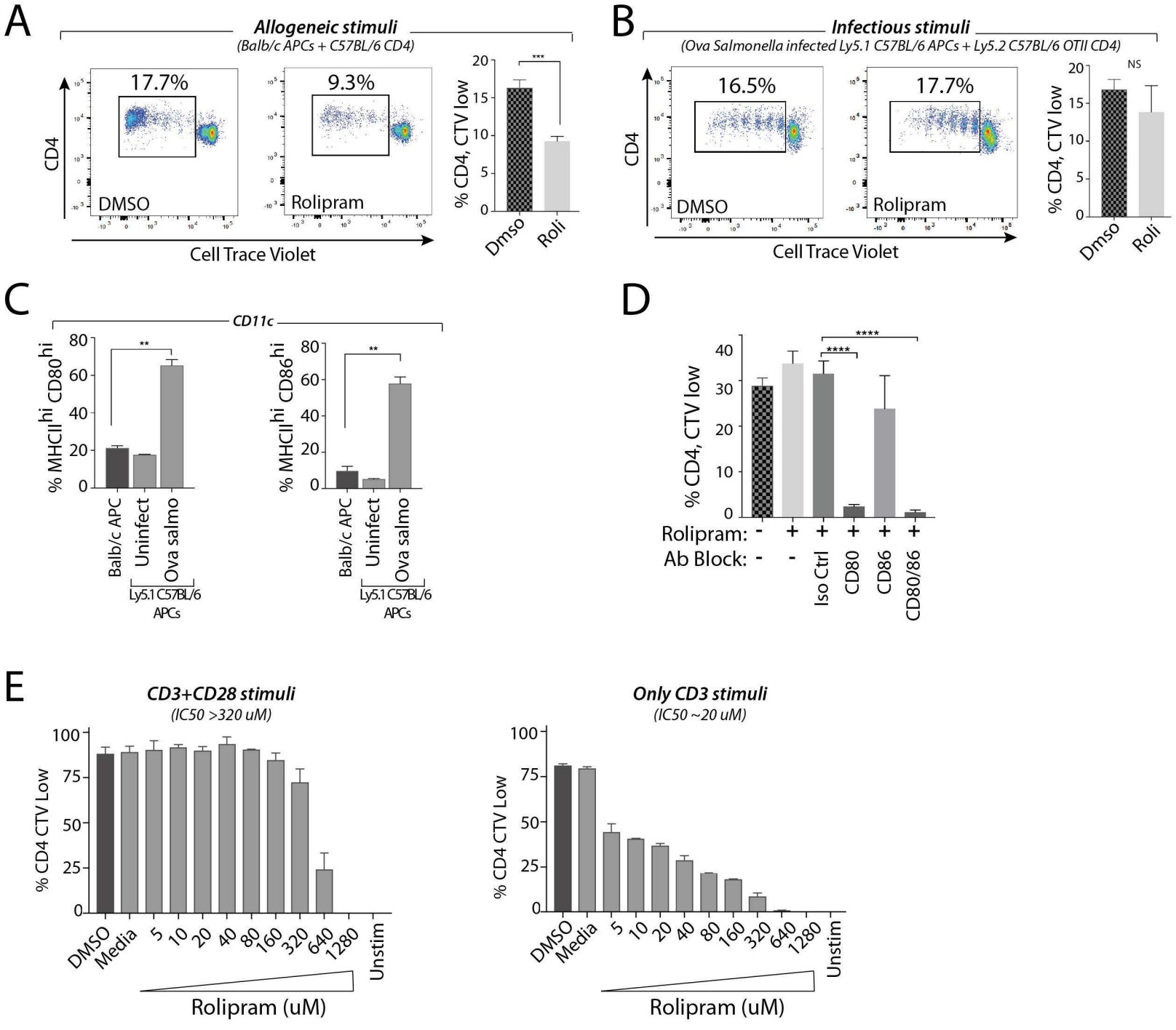
A
Allogeneic stimuli
(Balb/c APCs + C57BL/6 CD4)
17.7%
9.3%
CD4
DMSO
Rolipram
Cell Trace Violet
% CD4, CTV low
Dmso
Roli
B
Infectious stimuli
(Ova Salmonella infected Ly5.1 C57BL/6 APCs + Ly5.2 C57BL/6 OTII CD4)
16.5%
17.7%
NS
C
CD11c
% MHCII hi CD80 hi
% MHCII hi CD86 hi
Balb/c APC
Uninfect
Ova salmo
Ly5.1 C57BL/6 APCs
D
% CD4, CTV low
Rolipram:
Ab Block:
Iso Ctrl
CD80
CD86
CD80/86
E
CD3+CD28 stimuli
(IC50 >320 uM)
Only CD3 stimuli
(IC50 ~20 uM)
% CD4 CTV Low
DMSO
Media
Unstim
Rolipram (uM)

Figure 7

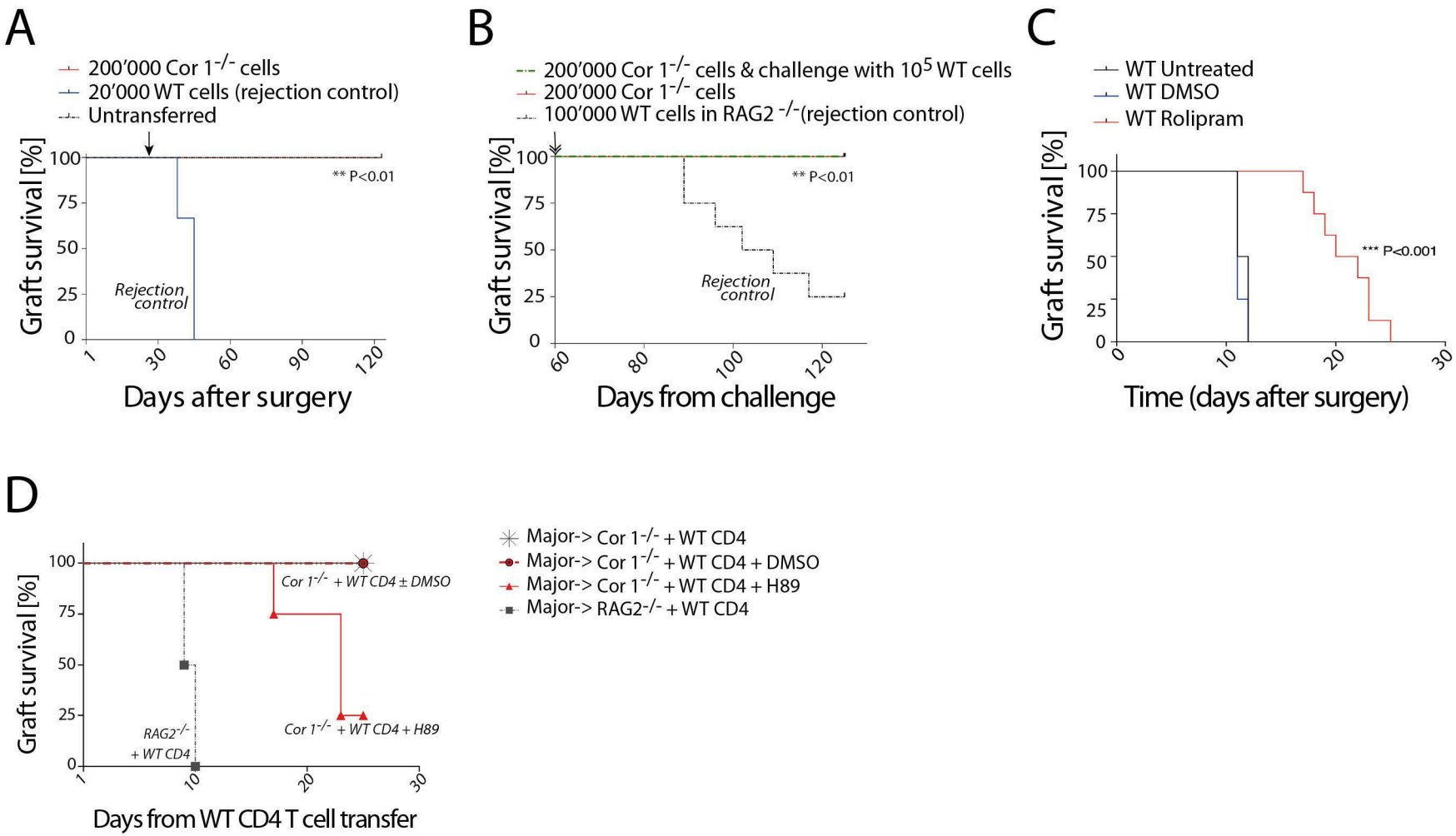
A
200'000 Cor 1-/- cells
20'000 WT cells (rejection control)
Untransferred
Graft survival [%]
100
75
50
25
0
** P<0.01
Rejection control
1
30
60
90
120
Days after surgery
B
200'000 Cor 1-/- cells & challenge with 10^5 WT cells
200'000 Cor 1-/- cells
100'000 WT cells in RAG2 -/-(rejection control)
Graft survival [%]
** P<0.01
Rejection control
60
80
100
120
Days from challenge
C
WT Untreated
WT DMSO
WT Rolipram
Graft survival [%]
*** P<0.001
0
10
20
30
Time (days after surgery)
D
Graft survival [%]
Cor 1-/- + WT CD4 ± DMSO
RAG2-/- + WT CD4
Cor 1-/- + WT CD4 + H89
Days from WT CD4 T cell transfer
Major-> Cor 1-/- + WT CD4
Major-> Cor 1-/- + WT CD4 + DMSO
Major-> Cor 1-/- + WT CD4 + H89
Major-> RAG2-/- + WT CD4

Figure S1

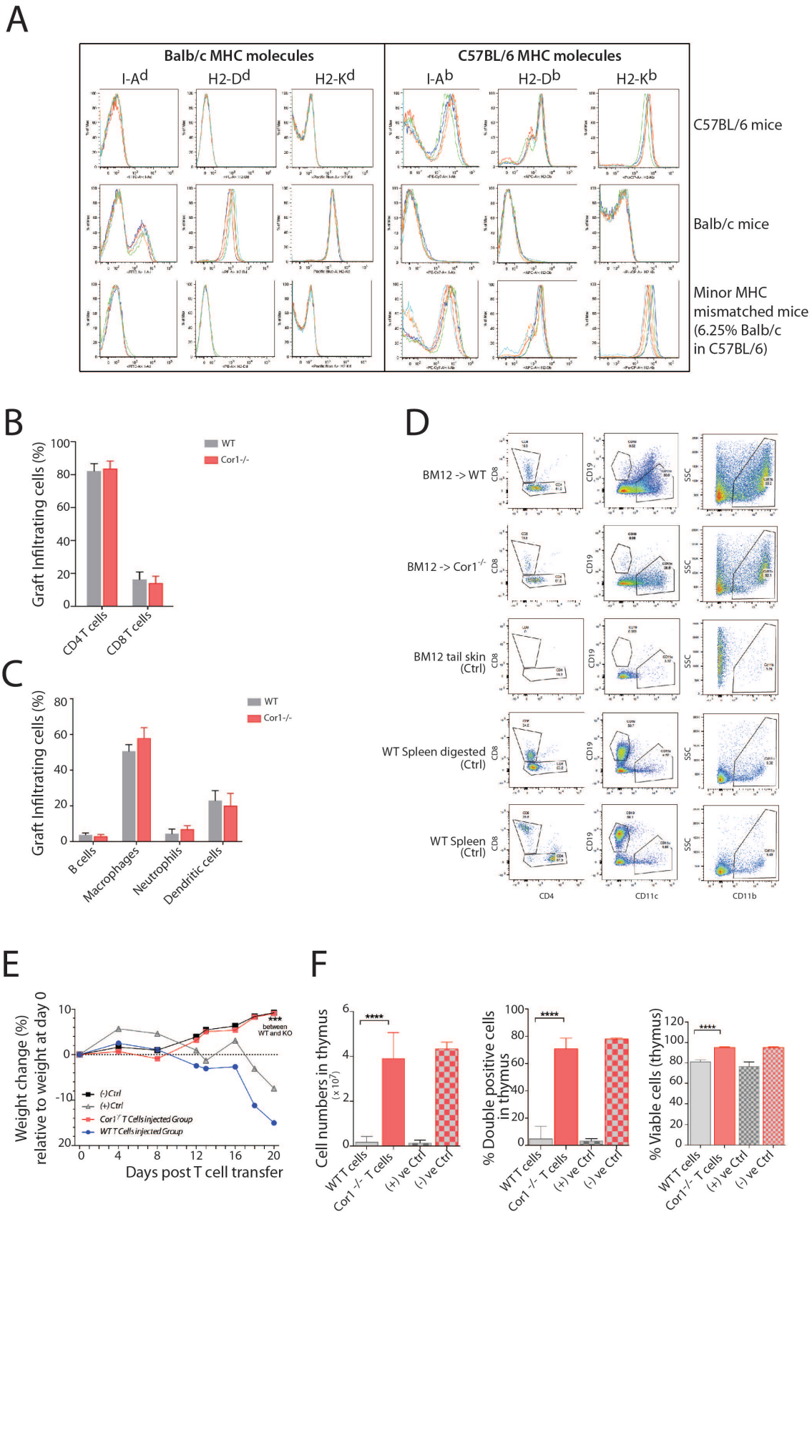
A
Balb/c MHC molecules
C57BL/6 MHC molecules
I-Ad
H2-Dd
H2-Kd
I-Ab
H2-Db
H2-Kb
C57BL/6 mice
Balb/c mice
Minor MHC mismatched mice (6.25% Balb/c in C57BL/6)
B
Graft Infiltrating cells (%)
WT
Cor1-/-
CD4 T cells
CD8 T cells
C
Graft Infiltrating cells (%)
WT
Cor1-/-
B cells
Macrophages
Neutrophils
Dendritic cells
D
BM12 -> WT
BM12 -> Cor1-/-
BM12 tail skin (Ctrl)
WT Spleen digested (Ctrl)
WT Spleen (Ctrl)
CD8
CD19
SSC
CD4
CD11c
CD11b
E
Weight change (%) relative to weight at day 0
Days post T cell transfer
***
between WT and KO
(-) Ctrl
(+) Ctrl
Cor1-/- T Cells injected Group
WT T Cells injected Group
F
Cell numbers in thymus (x 10^7)
% Double positive cells in thymus
% Viable cells (thymus)
****
WT T cells
Cor1-/- T cells
(+) ve Ctrl
(-) ve Ctrl

Figure S1: Characterization of minor histocompatibility antigen-mismatched mouse line, allograft immune cell infiltration and graft-versus-host responses. Related to Figure 1

(A) Characterization of minor histocompatibility antigen-mismatched mouse line for major histocompatibility complexes (see materials and methods for more details). Blood cells were stained with anti- I-A^b, H2-D^b, H2-K^b, I-A^d, H2-D^d and H2-K^d antibodies and analyzed by flow cytometry. n=5 mice per group. Two independent experiments. Left Panels: An antibody staining for BALB/c specific MHC complexes: I-A^d (MHC class II), H2-D^d and H2-K^d (MHC class I). Right panels: An antibody staining for C57BL/6 specific MHC complexes: I-A^b (MHC class II), H2-D^b and H2-K^b (MHC class I). n=5 mice per group.
(B-D) Immune cell infiltration: B, CD4 and CD8 T cell infiltration (CD3 gated) and C, B cells, macrophages, dendritic cell and neutrophil infiltration inside BM12 allograft on wild type and coronin$1^{-/-}$ mice as analyzed by flow cytometry. D: Representative FACS gating profiles for the indicated immune cells infiltrating the BM12 tail skin allograft onto wild type and coronin$1^{-/-}$ mice.
(E) Coronin 1 and graft versus host responses. Left panel: assessment of weight loss as a measure of graft versus host disease post adoptive transfer of 20 x 10^6 wild type or coronin 1-deficient T cells. BDF1 (I-A^{bd}) mice receiving total splenocytes, either from C57BL/6 (I-A^b) Ly5.1 mice or BDF1 (I-A^{bd}) mice served as positive and negative controls, respectively. Kinetics of weight loss relative to day 0, represented as percentage weight loss over a period of 20 days. P values (*** $p<0.001$) were calculated using unpaired Student's *t*-test. n= 7 mice per genotype. Two independent experiments.
(F) Flow cytometric analysis of cell numbers (*left panel*), double positive thymocytes (*middle panel*) and percentage viable cells (*right panel*) in thymus of BDF1 (I-A^{bd}) mice, three weeks post adoptive transfer of wild type or coronin 1-deficient T cells (20 x 10^6 wild type or coronin $1^{-/-}$ T cells (I-A^b) by FACS. BDF1 mice receiving total splenocytes, either from C57BL/6 (I-A^b) Ly5.1 mice (acute GvHD control) or BDF1 (I-A^{bd}) mice (no GvHD control) served as positive and negative controls, respectively. P values (**** $p<0.0001$), unpaired Student's *t*-test. n= 7 mice/genotype. Two independent experiments.

Figure S2

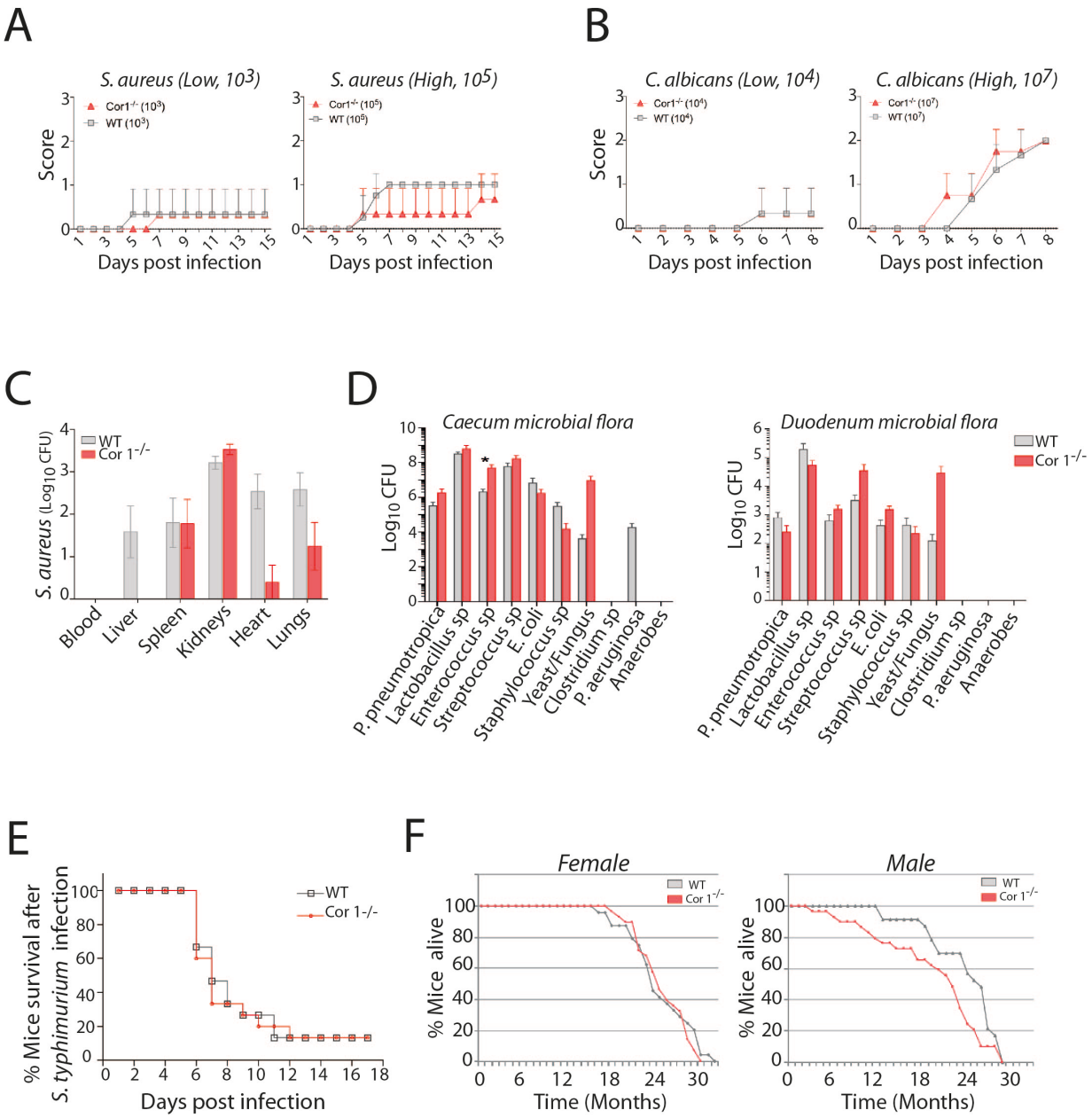

Figure S2: Coronin 1-deficient mice control infections comparable to wild type mice and have normal life span. Related to Figure 2

(A,B) Wild type or coronin $1^{-/-}$ mice were infected with a defined inoculum of *S. aureus* SA113 (4.8×10^3 or 4.8×10^5 CFU inoculum, (A) or *C. albicans* SC5314 (10^4 or 10^7 CFU inoculum, (B) using a subcutaneous catheter model and the mice were scored for the kinetics of disease progression. Score 0: No abscess, score 1: slight edema, no abscess, score 2: abscess ≤ 3 mm (diameter 6 mm), score 4: abscess≥ 3 mm (diameter 6 mm). n= 8-10 mice per genotype. From two independent experiments. No statistical significance was observed.

(C) *S. aureus* chronic infection model (Ziegler et al., 2011). Wild type or coronin $1^{-/-}$ mice were infected i.v. with $4x10^7$ CFU of *S. aureus* (strain SH1000) and on day 21 mice were sacrificed and the indicated organs collected aseptically, homogenized and various dilutions plated on agar plates and the CFU enumerated. n= 8 for wild type mice and n= 6 for coronin 1-deficient mice.

(D) Age and sex-matched mice (> 30 weeks) were sacrificed and caecal (left panel) and duodenal (right panel) suspensions plated on defined agar plates and cultured under aerobic or anaerobic conditions. Colonies were further characterized and CFUs enumerated. n=9 mice per genotype. From three independent experiments. P values (* $p<0.05$, ** $p<0.01$), unpaired Student's *t*-test. Similar profiles seen from duodenum and stomach.
(E) Wild type or coronin $1^{-/-}$ mice were infected orally with virulent *S. typhimurium* (10^6 bacilli, oral route) and the progression of disease (surface body temperature) and kinetics of mouse survival monitored. n=15 mice per genotype.
(F) Life span of wild type and coronin $1^{-/-}$ mice. Wild type and coronin $1^{-/-}$ mice (40 males and 40 females each genotype) were monitored until they became moribund. The values represent the survival span normalized to percentage and plotted over time. When moribund, mice were sacrificed and internal organs analyzed for organomegaly, lymphadenopathy, hemorrhagic ascites and other signs of malignant transformation. The coronin $1^{-/-}$ males are more aggressive (Jayachandran et al., 2014) and due to infighting displayed an altered survival curve.

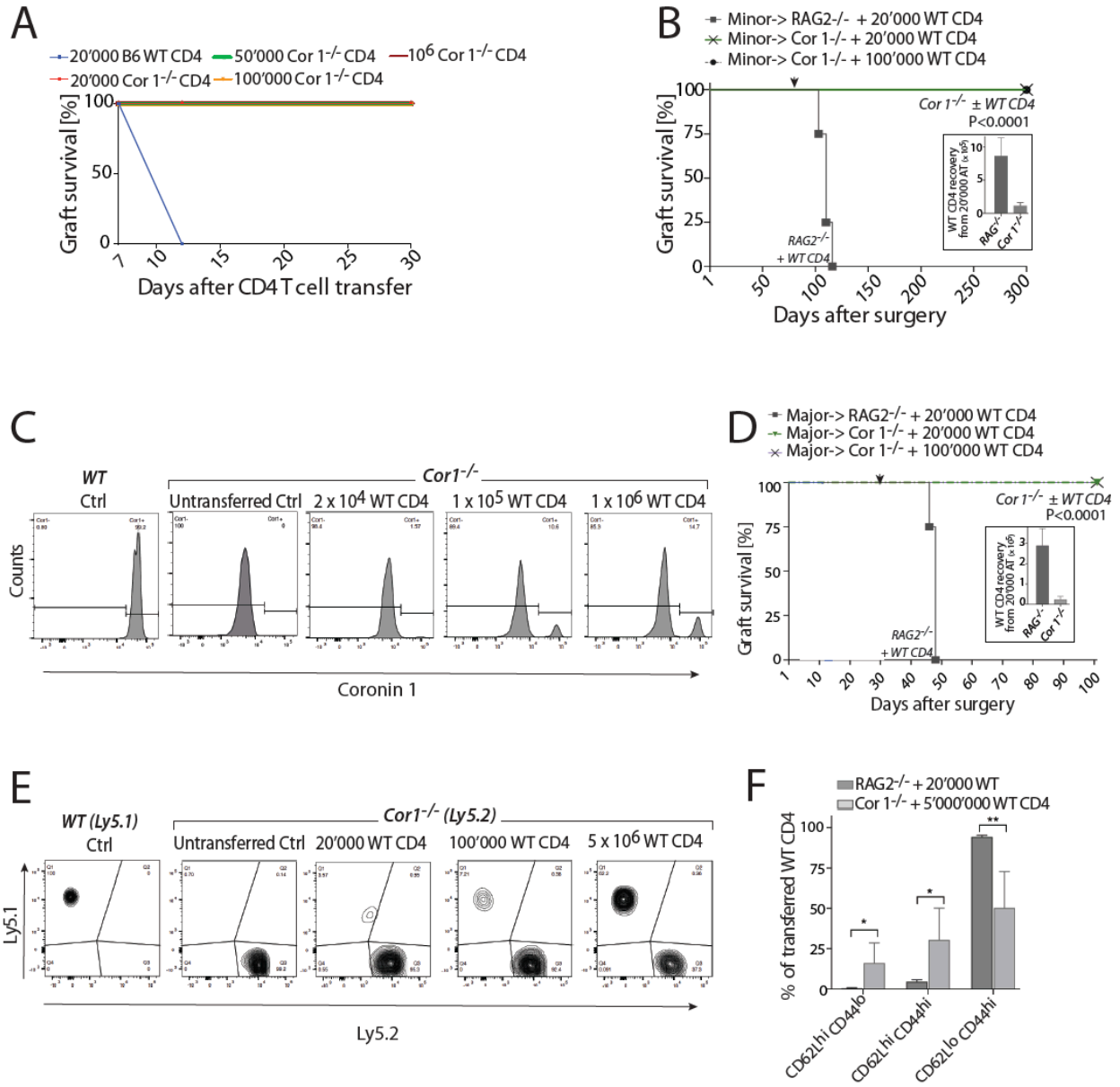

Figure S3: Coronin 1 deficiency actively suppresses wild type T cells from expansion and allorejection. Related to Figure 3

(A) Survival of BM12 RAG2$^{-/-}$ skin grafts in RAG2$^{-/-}$ recipients after transfer of wild type C57BL/6 and coronin 1$^{-/-}$ CD4^{+} T lymphocytes. Following transplantation, the recipient mice were adoptively transferred with CD4^{+} T cells i.v. on day 30 day (arrow). n= 5 mice/group. Two independent experiments.
(B) Survival of minor histocompatibility antigen-mismatched skin grafts transplanted onto coronin 1$^{-/-}$ (Cor 1$^{-/-}$) mice followed by adoptive transfer (AT) of wild type (20'000 and 10^{5}) CD4^{+} T cells. Arrow represents the time of AT. n=5 mice for minor-> wild type group and minor-> RAG2$^{-/-}$ group. n=8 mice for 20'000, 6 mice for 10^{5} CD4^{+} T cell transferred group. The RAG2$^{-/-}$ curves are from same cohort as shown in Fig 3A. *Inset:* Total wild type CD4^{+} T cells recovered from adoptive transfer of 20'000 wild type CD4^{+} T cells transfer in to RAG2$^{-/-}$ and Cor 1$^{-/-}$ mice on termination day.
(C) Flow cytometric analysis for the presence of adoptively transferred wild type CD4^{+} T cells in peripheral blood of coronin 1-deficient recipient mice by coronin 1 staining (rabbit anti-coronin 1, serum 320) on day 160. Shown are representative histograms for the groups adoptively transferred with various numbers of wild type CD4^{+} T cells. The data shown are for the T cells within the CD3^{+}CD4^{+} gate.

(D) Survival of major MHC mismatched skin grafts (BM12 skin grafts, I-A^{bm12}) transplanted onto Ly5.2 coronin $1^{-/-}$ mice (I-A^{b}) followed by adoptive transfer of Ly5.1 wild type (20'000 and 10^5) $CD4^+$ T cells. The arrow represents the time of adoptive transfer. At the time of transfer, as a control, 20'000 Ly5.1 wild type $CD4^+$ T cells were transferred into $RAG2^{-/-}$ mice bearing allografts (rejection control). Note: The traces from the coronin $1^{-/-}$ groups overlap. **** $P<0.0001$. Log-rank test between $RAG2^{-/-}$ and coronin $1^{-/-}$ mice receiving wild type $CD4^+$ cells. Representative of three independent experiments. n=9 mice for 20'000 group, 7 mice for 10^5 $CD4^+$ group, n=4 mice for rejection control BM12-WT group and 5 for control BM12-$RAG2^{-/-}$ group. The $RAG2^{-/-}$ curves are from the same cohort as shown in Fig 3B. *Inset*: Total wild type $CD4^+$ T cells recovered from adoptive transfer of 20'000 wild type $CD4^+$ T cells transfer into $RAG2^{-/-}$ and Cor $1^{-/-}$ mice on termination day.

(E) Flow cytometric analysis for the presence of adoptively transferred wild type Ly5.1 $CD4^+$ T cells in peripheral blood of coronin 1-deficient recipient mice (Ly5.2) on day 70 post adoptive transfer. Shown are representative contour plots for the groups adoptively transferred with various numbers of wild type Ly5.1 wild type $CD4^+$ T cells. The data shown are for the T cells within the $CD3^+CD4^+$ gate.

(F) Analysis of the adoptively transferred wild type $CD4^+$ T cells from coronin $1^{-/-}$ mice (shown in 3B) from the blood by flow cytometry for activation markers on day 70.

Figure S4

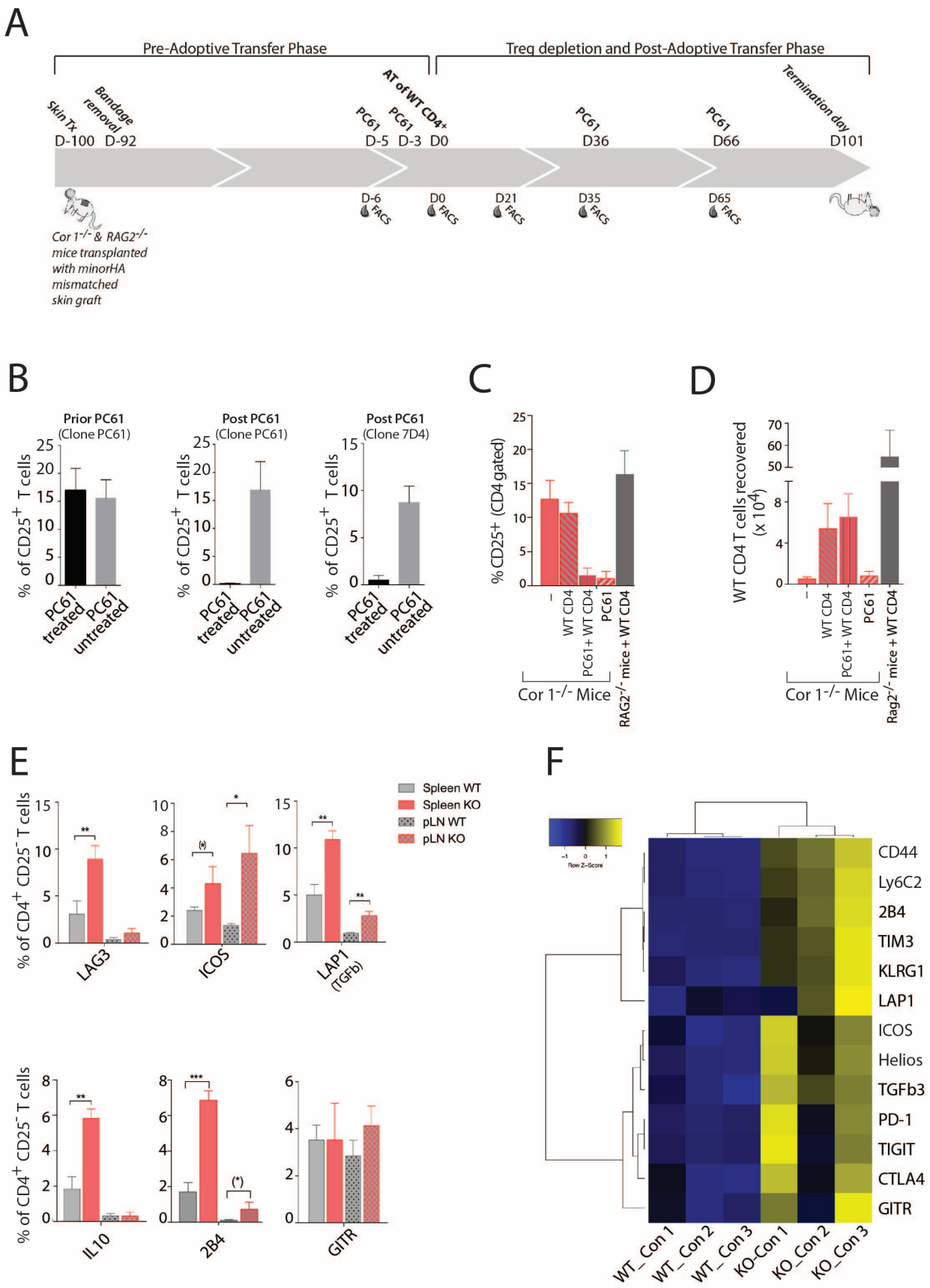
A
Pre-Adoptive Transfer Phase
Treg depletion and Post-Adoptive Transfer Phase
Skin Tx
Bandage removal
AT of WT CD4+
PC61
PC61
PC61
PC61
Termination day
D-100
D-92
D-5
D-3
D0
D36
D66
D101
D-6 FACS
D0 FACS
D21 FACS
D35 FACS
D65 FACS
Cor 1-/- & RAG2-/- mice transplanted with minorHA mismatched skin graft
B
Prior PC61 (Clone PC61)
Post PC61 (Clone PC61)
Post PC61 (Clone 7D4)
% of CD25+ T cells
PC61 treated
PC61 untreated
C
% CD25+ (CD4 gated)
WT CD4
PC61+ WT CD4
PC61
RAG2-/- mice + WT CD4
Cor 1-/- Mice
D
WT CD4 T cells recovered (x 10^4)
Rag2-/- mice + WT CD4
Cor 1-/- Mice
E
Spleen WT
Spleen KO
pLN WT
pLN KO
% of CD4+ CD25- T cells
LAG3
ICOS
LAP1 (TGFb)
IL10
2B4
GITR
F
Row Z-Score
CD44
Ly6C2
2B4
TIM3
KLRG1
LAP1
ICOS
Helios
TGFb3
PD-1
TIGIT
CTLA4
GITR
WT_Con 1
WT_Con 2
WT_Con 3
KO-Con 1
KO_Con 2
KO_Con 3

Figure S4: Coronin 1-deficient conventional T cells are alloprotective and have an immunosuppressive phenotype. Related to Figure 3

(A) Scheme of the experimental setup for the analysis of the role of $CD25^+$ Tregs in the context of minor histocompatibility antigen-mismatched skin transplant rejection. Coronin $1^{-/-}$ mice and $RAG2^{-/-}$ controls that had been transplanted with minor histocompatibility antigen-mismatched skin transplant were subjected to anti-CD25 antibody (clone PC61, 0.5 mg/mouse IP) administration to deplete regulatory T cells (on D-5, D-3, D36 and D66) followed by AT of wild type $CD4^+CD25^-$ T cells (on D0, tail vein) and kinetics of graft rejection monitored. Mice were bled on various days (D-5, D0, D21, D35 and D65) to assess the efficacy of PC61 mediated $CD25^+$ T cell depletion by anti-CD25 antibody (clone 7D4).
(B) Assessment of efficacy of depletion of $CD4^+CD25^+$ T cells (Tregs) following PC61 depletion. Mice were split into two groups (PC61 treated and PC61 untreated) and their tail vein blood assessed prior (left panel) and post (middle and right panel) PC61 administration for $CD4^+CD25^+$ status using the anti-mouse CD25 antibody clone PC61 (left and middle panel) and clone 7D4 (right panel). n=15 mice for PC61 treated and 9 for PC61 untreated.
(C) Assessment of efficiency of CD25 depletion by anti-CD25 clone 7D4 at the time of study termination shown in Figure 3C,D from spleen and lymph nodes.
(D) Enumeration of transferred wild type $CD4^+$ T cells from spleen, lymph nodes and blood of coronin $1^{-/-}$ mice by flow cytometry at the time of study termination shown in Figure 3C,D.
(E) Analysis of markers on $CD4^+$ T cells isolated from the spleen and peripheral lymph nodes (pLN; axillary and inguinal) of wild type and coronin $1^{-/-}$ mice by flow cytometry. LAG3; Lymphocyte Activation Gene 3; ICOS; Inducible T-cell CO-Stimulator; LAP1; Latency-Associated Peptide 1; IL10; Interleukin 10 and GITR; Glucocorticoid-Induced TNFR family Related gene. Levels of CTLA4, TIM3 and Helios were found to be comparable (not shown). * $P<0.05$, ** $P<0.01$. Unpaired Student's *t*-test. n=3 mice per genotype. Three independent experiments.
(F) Heatmap showing the expression of exhaustion markers that are differentially expressed in wild type versus coronin 1-deficient conventional T cells (see Table S3). Abundance estimates are represented as counts per million as per Robinson et al. (Robinson et al., 2010). Hierarchical clustering was computed in R using Pearson correlation distance and Ward D2 agglomeration.

Figure S5

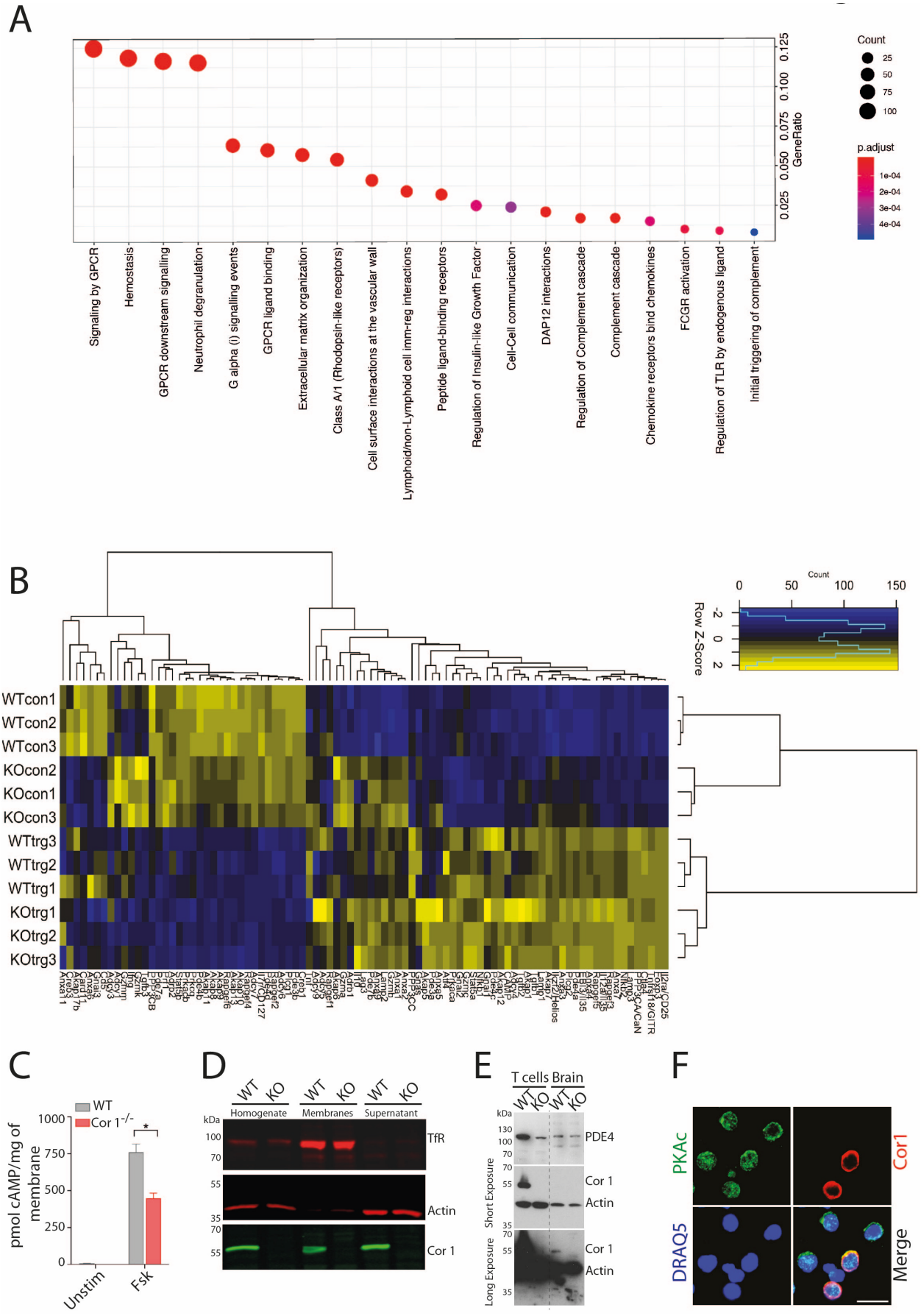
A
Count
25
50
75
100
p.adjust
1e-04
2e-04
3e-04
4e-04
GeneRatio
0.025
0.050
0.075
0.100
0.125
Signaling by GPCR
Hemostasis
GPCR downstream signalling
Neutrophil degranulation
G alpha (i) signalling events
GPCR ligand binding
Extracellular matrix organization
Class A/1 (Rhodopsin-like receptors)
Cell surface interactions at the vascular wall
Lymphoid/non-Lymphoid cell imm-reg interactions
Peptide ligand-binding receptors
Regulation of Insulin-like Growth Factor
Cell-Cell communication
DAP12 interactions
Regulation of Complement cascade
Complement cascade
Chemokine receptors bind chemokines
FCGR activation
Regulation of TLR by endogenous ligand
Initial triggering of complement
B
Count
0
50
100
150
Row Z-Score
-2
0
2
WTcon1
WTcon2
WTcon3
KOcon2
KOcon1
KOcon3
WTtrg3
WTtrg2
WTtrg1
KOtrg1
KOtrg2
KOtrg3
C
WT
Cor 1 -/-
pmol cAMP/mg of membrane
1000
750
500
250
0
*
Unstim
Fsk
D
WT
KO
Homogenate
Membranes
Supernatant
kDa
100
70
55
35
TfR
Actin
Cor 1
E
T cells
Brain
WT
KO
kDa
130
100
70
55
35
PDE4
Cor 1
Actin
Short Exposure
Long Exposure
F
PKAc
Cor1
DRAQ5
Merge

Figure S5: Coronin 1 deficiency alters cAMP signaling in T cells. Related to Figure 4

(A) Dot plot showing the most significantly enriched pathways among the differentially expressed genes in wild type versus coronin 1-deficient conventional T cells for the Reactome Pathways collection (Yu and He, 2016; Yu et al., 2012). P-values were adjusted using the Benjamini-Hochberg procedure. The background set of genes (universe) was the ~15000 genes detected in the RNA-Seq experiments.
(B) Heatmap of significantly differentially expressed genes with functions related to cAMP signaling. Regularized log-transformed (rlog) expression values were calculated in DESeq2 (Love et al., 2014) and hierarchically clustered using Pearson correlation with average linkage as implemented in R.
(C) Equal amount of membranes from wild type or coronin $1^{-/-}$ Jurkat T cells were stimulated with 100 μM forskolin (FSK) for 15 min at RT and the amount of cAMP determined by cAMP ELISA. n= 4 independent experiments. P values (* $p<0.05$) unpaired Student's *t*-test.
(D) Equal amount of total homogenate, membranes or the supernatant obtained from ultracentrifugation steps from wild type or coronin 1-defcient Jurkat T cells were probed for transferrin receptor (TfR, membrane marker), actin (cytosol) and coronin 1 by Western blotting using IR labeled secondary antibodies and imaged using a LI-COR system.
(E) Equal protein amounts from lysates of T cells or brain of wild type and coronin $1^{-/-}$ mice were immunoblotted for PDE4, coronin 1 and actin. For convenience, a dotted line has been inserted between the T cell and brain samples. For coronin 1, both a short and long exposure of the immunoblot is shown. Representative blot from two independent experiments.
(F) T cells from wild type and coronin 1-deficient spleens were mixed in a 1:1 ratio on a coverslip and stained using antibodies against the catalytic subunit of PKA (PKAc) along with anti-coronin 1 anti-serum (1002) and DRAQ5 and imaged using a laser scanning confocal microscope. Representative images from at least two independent experiments. Scale bar = 10 μm.

Figure S6

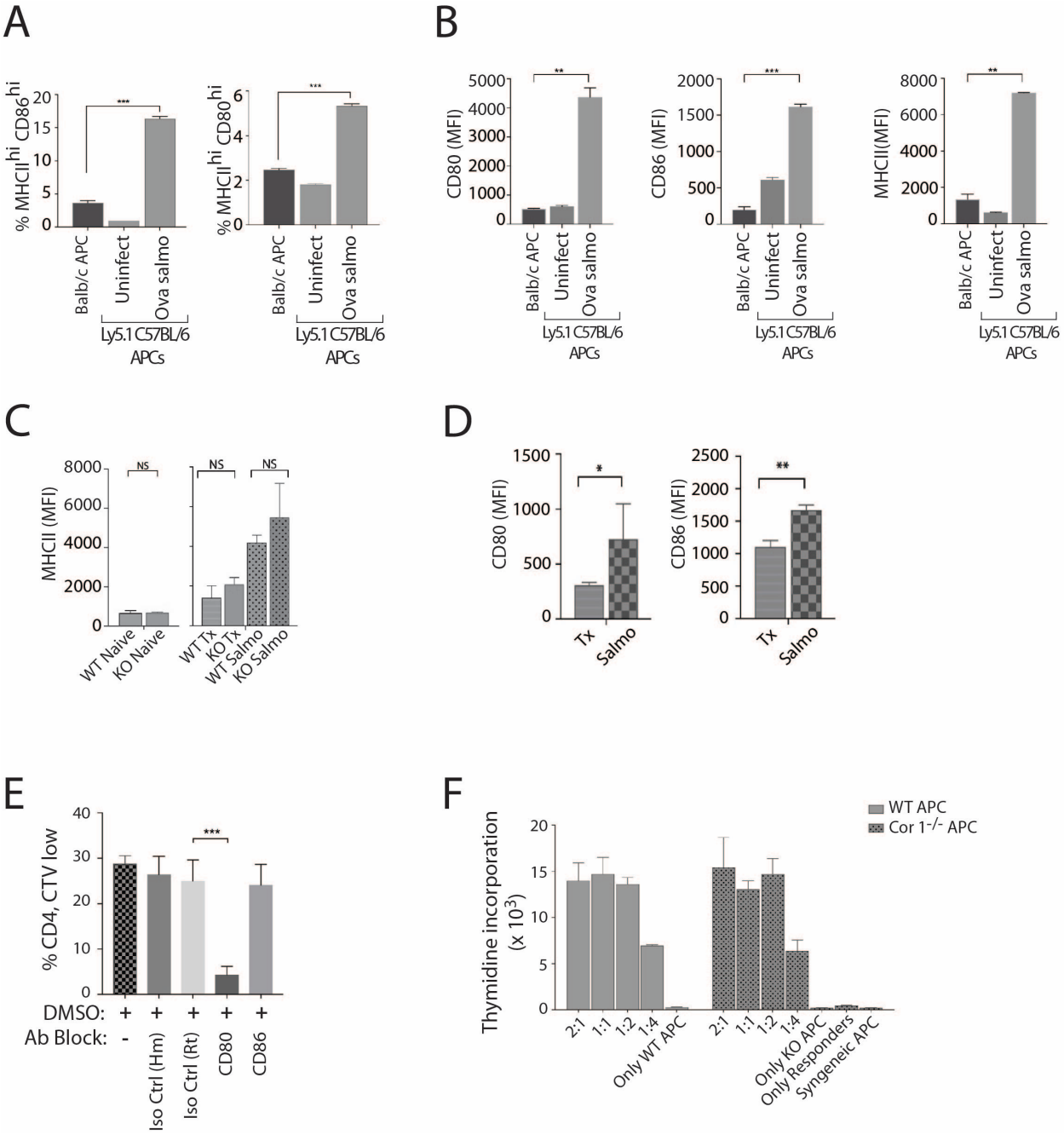

Figure S6: Enhanced induction of MHC class II and co-stimulatory molecules upon infection and similar MLR responces triggered by wild type and coronin 1-deficient APC's. Related to Figure 6

(A) Total APCs from spleen of Balb/c (I-A^d) and C57BL/6 (I-A^b) mice analyzed for expression of indicated co-stimulatory molecules. *Left panel;* % of APCs MHCII^{hi}CD86^{hi}. *Right panel;* % of APCs MHCII^{hi}CD86^{hi}.
(B) APCs isolated from spleens of Balb/c (I-A^d) and C57BL/6 (I-A^b) mice were either left uninfected or infected with Ova-*Salmonella* and analyzed 24 h later by flow cytometry for Median Fluorescence Intensity (MFI) of CD80, CD86 and MHCII from CD11c gated population. ** P<0.01, *** P<0.001. Unpaired *t*-test. Three independent experiments.
(C) APCs isolated from the draining lymph nodes of wild type or coronin 1-deficient mice that were challenged with either allo- (BM12) or microbial (*Salmonella*) antigens and analyzed, 7 or 4 days later

respectively, by flow cytometry for Median Fluorescence Intensity (MFI) of MHCII from CD11c gated population. No statistically significant difference noted. Unpaired *t*-test.
(D) APCs isolated from the draining lymph nodes of C57BL/6 mice that were challenged with either allo- (BM12) or microbial (*Salmonella*) antigens and analyzed, 7 or 4 days later respectively, by flow cytometry for Median Fluorescence Intensity (MFI) of CD80 and CD86 from the CD11c gated population. * $P<0.05$, ** $P<0.01$. Unpaired *t*-test.
(E) Analysis of wild type OTII CD4 T cell (C57BL/6 (I-A^b)) proliferation upon co-incubation with APCs (C57BL/6 (I-A^b)) that had been priorly infected with Ova-*Salmonella* in the presence of the indicated antibodies and DMSO. Shown are the percentage of cells that are CTV low from triplicate samples. *** $P<0.0001$. Unpaired Student's *t*-test. Hm; hamster control. Rt; rat control, Iso; Isotype.
(F) Mixed lymphocyte reaction was performed with APCs isolated from wild type or coronin 1-deficient C57BL/6 (I-A^b) mice in the presence of wild type T cells isolated from Balb/c (I-A^d) mice. After co-incubation for 3 days, 1 μCi of ^{3}[H]-thymidine was added and further incubated for 20h and DNA incorporated counts measured. Triplicate measurements and shown is the SD. No statistical differences.

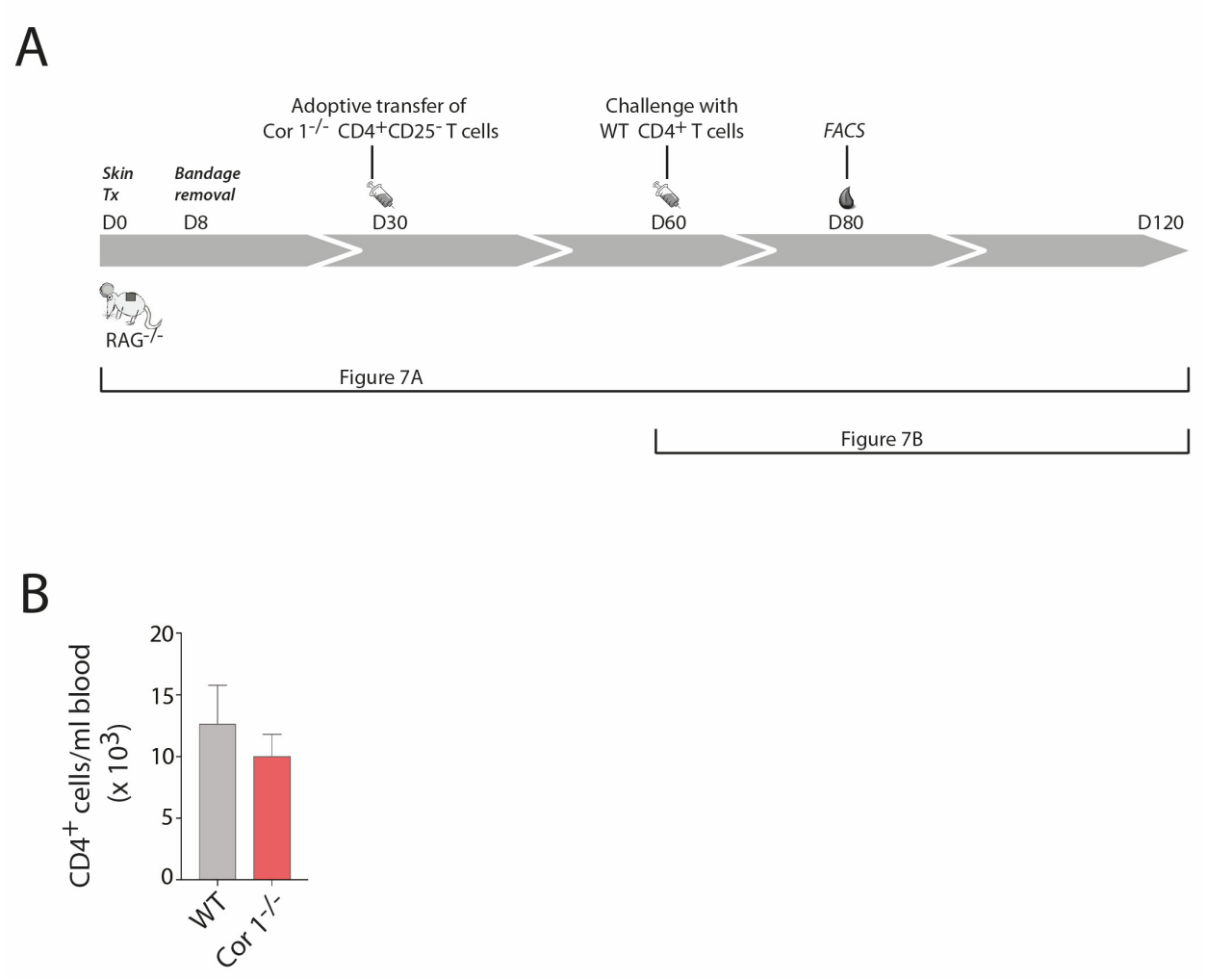

Figure S7: Outline of tolerance induction through the prior transfer of coronin 1-deficient T cells and confirmation of the presence of subsequently transferred wild type allo-reactive cells. Related to Figure 7

A) Scheme of the experimental setup for the analysis of the allograft tolerance induction by coronin 1-deficient $CD4^{+}CD25^{-}$ conventional T cells in the context of minor histocompatibility antigen- mismatched skin transplant rejection. $RAG2^{-/-}$ mice that had been transplanted with skin graft (D0) were subjected to adoptive transfer of coronin 1-deficient T $CD4^{+}CD25^{-}$ T cells (200'000 cells) or wild type $CD4^{+}$ T cells (20'000 cells, positive control) on D30, or left un-transferred and kinetics of graft rejection monitored. On day 60, those mice that received coronin 1-deficient $CD4^{+}CD25^{-}$ T cells were challenged with wild type $CD4^{+}$ T cells (D60, 100'000 cells) or left un-transferred and kinetics of graft rejection monitored. Mice were bled to confirm the presence of transferred cells on D80. $RAG2^{-/-}$ mice carrying a minor BALB/c ($I\text{-}A^{d}$) allograft and adoptively transferred only with wild type $CD4^{+}$ T cells (100'000 cells) on D60 served as controls for transfer and cell viability.
(B) Enumeration of wild type and coronin 1-deficient $CD4^{+}$ T cells from $RAG2^{-/-}$ mice adoptively transferred with coronin 1-deficient $CD4^{+}CD25^{-}$ T cells followed by challenge with wild type $CD4^{+}$ T cells. Flow cytometry was performed three weeks after challenge with wild type $CD4^{+}$ T cells (D80).

Table S1: Related to Figure 2. Analysis of aged mice, microbiological status: Virus and parasites

Serological analysis

		WT (Positive/total)	Cor1 $^{-/-}$(Positive/total)	Method
Viruses	Ectromelia virus	0/6	0/6	IFA
	Lymphocytic choriomeningitis virus (LCMV)	0/6	0/6	IFA
	Mouse adneovirus, FL	0/6	0/6	ELISA
	Mouse adenovirus, K87	0/6	0/6	ELISA
	Mouse cytomegalovirus (MCMV)	0/6	0/6	ELISA
	Mouse rota virus (EDIM)	0/6	0/6	IFA
	Mouse hepatitis virus (MHV)	0/6	0/6	IFA
	Murine Norovirus (MNV)	4/6	0/6	PCR / IFA
	Mouse parvo virus (MPV)	0/6	0/6	IFA
	Minute virus of mice (MVM)	0/6	0/6	IFA
	Pneumonia virus of mice (PVM)	0/6	0/6	IFA
	Reovirus type 3	0/6	0/6	IFA
	Sendai virus	0/6	0/6	IFA
	Theiler's murine encephalomyelitis virus (TMEV)	0/6	0/6	IFA
Mycoplasma	Mycoplasma pulmonis	0/6	0/6	IFA
Bacteria	Chlostridium piliforme	0/6	0/3	ELISA / IFA
	Helicobacter Sp	0/6	0/6	PCR
Parasites	Endoparasites/Protozoan	2/6 (Chilomastix sp), 2/6 (Hexamastix)	6/6 (Trichomonas sp), 2/6 (Hexamastix sp)	

n=6 mice per genotype

IFA: Indirect Fluorescence Analaysis

PCR: Polymerase Chain Reaction

ELISA: Enzyme Linked Immuno Sorbent Assay

Table S2:Related to Figure 2. Blood biochemistry of Coronin 1-deficient mice (young and aged).

Table 1a	Aged Mice				Young Mice			
Parameter	**WT**	***Stdev WT***	**Cor1**-/-	***Stdev KO***	**WT**	***Stdev WT***	**Cor1**-/-	***Stdev KO***
Sodium (mmol/l)	151.67	*1.53*	154.00	*1.00*	156.64	*2.06*	154.45	*1.21*
Potassium (mmol/l)	10.17	*0.67*	9.93	*1.91*	5.41	*0.46*	5.93	*0.61*
Chloride (mmol/l)	112.33	*0.58*	116.67	*3.79*	105.27	*1.35*	106.09	*1.97*
Calcium (mmol/l)	2.66	*0.09*	2.60	*0.10*	1.97	*0.78*	2.33	*0.07*
Glucose (mmol/l)	8.23	*5.08*	11.66	*3.90*	5.06	*1.44*	6.85	*1.19*
Total Cholesterol (mmol/l)	2.10	*0.49*	1.95	*0.27*	2.31	*0.79*	2.68	*0.26*
HDL-Cholesterol (mmol/l)	1.42	*0.26*	1.28	*0.39*	2.36	*0.20*	2.52	*0.22*
Triglycerides (mmol/l)	1.20	*0.23*	1.36	*0.43*	1.34	*0.38*	0.98	*0.23*

Table 1b	Aged Mice			
Parameter	**WT**	***Stdev WT***	**Cor1**-/-	***Stdev KO***
Magnesium (mmol/l)	1.43	*0.15*	1.51	*0.23*
Phosphate (mmol/l)	2.77	*0.14*	2.66	*0.38*
Urea (mmol/l)	7.07	*0.57*	9.00	*1.85*
Uric Acid (μmol/l)	213.00	*8.49*	256.33	*63.85*
Creatinine (mmol/l)	8.67	*0.58*	11.33	*4.16*
Chol./HDL-Chol-Quotient	1.47	*0.15*	1.58	*0.28*
Total Protein (g/l)	55.50	*0.71*	51.67	*10.26*
Albumin (g/l)	14.13	*3.36*	14.54	*1.71*
Globulin (g/l)	39.50	*2.12*	32.50	*2.12*
ASAT (U/l)	243.00	*107.76*	187.00	*101.39*
ALAT (U/l)	52.00	*16.09*	93.67	*86.60*
GGT (U/l)	ND		<1	
Alk. Phosphatase (U/l)	78.00	*73.82*	104.67	*68.31*
Bilirubin (μmol/l)	1.90	*0.17*	2.24	*0.71*

n= 11 mice per genotype for young mice (<10 weeks)
n= 6 mice per genotype for aged mice (>30 weeks)